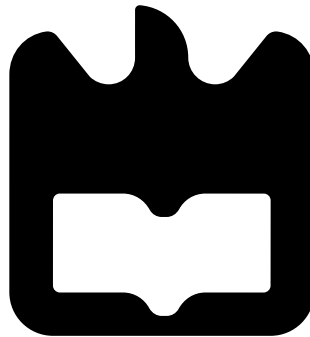**Eduardo Lima da Rocha Miranda**

Sistema de Monitorização de botijas de gás

Monitoring system for gas cylinders

**Eduardo Lima da
Rocha Miranda**

Sistema de Monitorização de botijas de gás

Monitoring system for gas cylinders

Dissertação apresentada à Universidade de Aveiro para cumprimento dos requisitos necessários à obtenção do grau de Mestre em Engenharia Electrónica e Telecomunicações, realizada sob a orientação cientica do Professor Dr. José Manuel Neto Vieira, Professor Auxiliar do Departamento de Electrónica, Telecomunicações e Informática da Universidade de Aveiro e do Professor Dr. Nuno Miguel Gonçalves Borges de Carvalho, Professor Auxiliar do Departamento de Electrónica, Telecomunicações e Informática da Universidade de Aveiro.

o júri / the jury

presidente / president

Professora Doutora Ana Maria Perfeito Tomé
Professora Associada da Universidade de Aveiro

vogais / examiners committee

Professor Doutor Salviano Filipe Silva Pinto Soares
Professor Auxiliar do Departamento de Engenharias da ECT da Universidade de Trás-os-Montes e Alto Douro (arguente principal)

Professor Doutor José Manuel Neto Vieira
Professor Auxiliar da Universidade de Aveiro (orientador)

Palavras-chave   Resposta Impulsional, Resposta em Frequência, sistemas LTI, método de Welch, Correlação

Resumo   As botijas de gás GPL (Gás de Petróleo Liquefeito) encontram-se em circulação há vários anos a fornecer serviço de gás para a população. Durante todos estes anos o mesmo problema persistiu, a falta de um método viável para medir o nível de líquido dentro de uma botija de gás que fosse automático e sem intervenção do utilizador. Se o distribuidor tivesse acesso ao nível de gás de cada botija numa base de dados, seria possível avisar o utilizador sobre o nível de gás dentro da botija e oferecer ao mesmo a troca da botija vazia por uma botija cheia, proporcionando uma nova forma de interação entre utilizador e distribuidor. Uma solução que poderia permitir este tipo de interação passa pelo desenvolvimento de um sistema de medição, simples e barato, para medir o nível de líquido de uma botija de gás e comunicar o seu estado, através de IoT (*Internet of Things*), a uma base de dados. Neste trabalho, é proposto um método para medir o nível de líquido de uma botija de gás tirando partido das frequências de ressonância da botija, que variam de acordo com o respetivo nível de líquido, o que torna possível o mapeamento do peso da botija, com a sua respetiva frequência.

Abstract   The LPG (Liquefied Petroleum Gas) cylinder is in circulation for many years, providing gas service for the population. During all those years the same problem persisted, the lack of a viable method to measure the liquid level inside a gas cylinder automatically and without the intervention of the user. If the distributor had access to the level of gas of each gas cylinder in a database, it would be possible to warn the user about the gas level and offer to trade the empty tank for a full one providing a new way of interaction between the user and the distributor. A solution that could enable this new interaction is the development of a simple and cheap measuring system to measure the liquid level and communicate its status, through IoT (*Internet of Things*), to a database. In this work, a way to measure the liquid level is proposed taking advantage of the resonant frequencies of the cylinder, which varies with the liquid level of gas. Therefore is possible to map the weight of the cylinder with its corresponding frequency.

Contents

List of Figures

iv

List of Tables

Acronyms

ADC Analog to Digital Converter.

DAC Digital to Analog Converter.

DTFT Discrete-Time Fourier Transform.

FET Field-Effect Transistor.

FFT Fast Fourier Transform.

IoT Internet of Things.

LPF Low Pass Filter.

LPG Liquefied Petroleum Gas.

LTI Linear and Time-Invariant.

MATLAB MATrix LABoratory.

PSD Power Spectrum Density.

RF Radio Frequency.

RMS Root Mean Square.

SI International System of Units.

Chapter 1

Introduction

1.1 Motivation

Currently, society is migrating to different types of energy less pollutant, being natural gas one of them. Natural gas produces less carbon dioxide per unit energy release when compared with other fossil fuels. The uses of natural gas vary to domestic, commercial and industrial applications such as cooking, heating and as an alternative to gasoline or diesel[1].

The problem with natural gas is that it comes from a distribution network that does not cover the entire population. An alternative is the use of Liquefied Petroleum Gas (LPG), also known as propane or butane.

The LPG cylinder is in circulation for many decades providing gas service for the population that still cannot use natural gas. The main problem with the use of an LPG cylinder is its management. It is not easy to accurately measure if the cylinder is near its end, leaving for the user discern if it is, or it is not, the time to change the used cylinder for a new one.

By providing the distributor with a network where it would be possible to store the value of each cylinder in utilization, a new way of interaction between the distributor and the user could be achieved.

So, It would be interesting to create a system to measure the liquid level of a gas cylinder and communicate its value, through the Internet of Things (IoT), to a database that would allow the distributor to warn the user about the liquid level of the cylinder and if it was time to change the tank.

The work developed in this master thesis is based on the experimental results of Wu et al[2], more specifically on the observation that the resonant frequency of a gas cylinder varies with the liquid level inside the cylinder.

Since the resonant frequency changes with the liquid level of the cylinder, it is possible to develop a way to measure the liquid level of gas cylinder mapping the weight of the cylinder with its corresponding frequency which allows its future integration with a simple low-cost sensor for a better management of a LPG cylinder.

1.2 Objectives

The objective of this work is the measurement of the liquid level of a gas cylinder, through analysis of the impulse and the frequency response of the cylinder for two methods, direct and indirect. The direct impulse response is acquired when the input signal is the knock of

a hammer, in contrast to a linear chirp, where is necessary to correlate the output with the input, being this method an indirect method for acquiring the impulse response. With the frequency response of each cylinder is possible to map the weight with the frequency with the higher magnitude and compare, for the two methods, if the linear chirp gives a response that is similar to the knock of a hammer.

1.3 Organization

This dissertation has the following organization:

- In Chapter 2 is presented all the theory that supports the experiments done on the subsequent chapters.

- In Chapter 3 is presented the experimental setup for the liquid level measurement of a gas cylinder as well the results obtained for the experiment when the input signal is the knock of a hammer. The Linearity of the system is also shown.

- In Chapter 4 is presented the experimental setup for the liquid level measurement of a gas cylinder as well as the results obtained when the input signal is a linear chirp.

- In Chapter 5 and as conclusion, the main results are presented and an improved model to measure the liquid level of a gas cylinder is proposed for future work.

Chapter 2

Liquid level detection techniques

2.1 Introduction

During the last few years, to measure the level of gas in a cylinder, it was necessary to use manual techniques (like weighing) or buy an external gauge[3] and install on it, in order to have a rough estimate on the level of gas and to decide if it was time to exchange it. The problem with this kind of measurement techniques is that they only provide a rough estimate. Thanks to this, it rests on the user discernment if he should buy a new one or not. To mitigate this problem and to measure the level of gas in a cylinder with more precision, several methods were proposed through the use of RF waves[4], acoustic waves[5] and ultrasonic waves[6]. The problem with these methods is the need to install a transmitter/receiver pair inside the top of the cylinder.

As the quantity of gas cylinders in circulation exists in great numbers, it's unpractical to install internal sensors in all of them. A solution was then proposed by Hsien-Huang P. Wu and Zong-Hao Yang[2] which consisted of continuous measurements by installing a knocking device outside the cylinder. With this method, it's possible to capture the generated frequencies that occur on the cylinder every time a knock happens.

This dissertation tries to replicate their work and enhance it a step further, replacing the knocking device with a more practical frequency sweep. To do that, first is necessary to understand the problem in hands.

2.2 System concept

In Engineering, it's possible to describe a system as a mathematical operator that transforms an input signal, usually known as $x(n)$, in an output signal $y(n)$ through the use of a set number of properties. Any system H can be represented as follow:
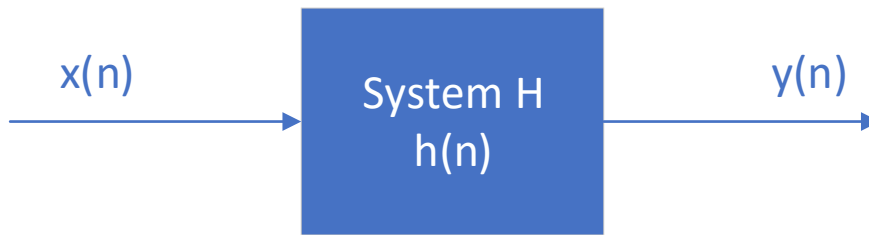
Figure 2.1: Block diagram of a generic discrete system.

This representation allows, in a systematic way, to understand how a system behaves according to possible environmental changes[7].

2.3 A mathematical model of a gas cylinder

2.3.1 Introduction

Being possible to describe a system through mathematical proprieties, if we consider our gas cylinder a system, it's possible to create a mathematical model to understand its behavior.

The first person to provide a useful model to the traverse vibration of a cylindrical tube filled with different liquid levels was K.T. Chan and J.Z. Zhang[8][2]. His model consisted on measuring the influence of the gas quantity in the tank to the resonant frequency, being the tube clamped at the bottom and free at the top (clamped-free model).

Positive results led Chan et al[8] to extend their model to the study of the vibration of a simply supported uniform beam partially loaded with a distributed mass (pinned-pined model), where is shown the calculus of the natural frequencies (or eigenfrequencies) and its related mode shape[9].

With an approach similar to Chan et al[8][9], but using different boundary conditions, Jacobs et al[10] presented a method which permitted a contactless measurement of thin liquid levels of a finite section of a tube through resonant frequencies, achieving results in accordance to the experimental data.

Finally, Wu et al[2] based their work on these previous studies proposing a model where Euler-Bernoulli beam theory could be used to explain the vibrations on a gas tank. Please refer to the appendix for the theoretical explanation of the Euler-Bernoulli beam theory.

2.3.2 Euler-Bernoulli on a gas cylinder

Trough the Euler-Bernoulli beam theory, a model for a gas cylinder partially filed, like the one showed in Figure 2.2, was proposed by Wu et al[2].
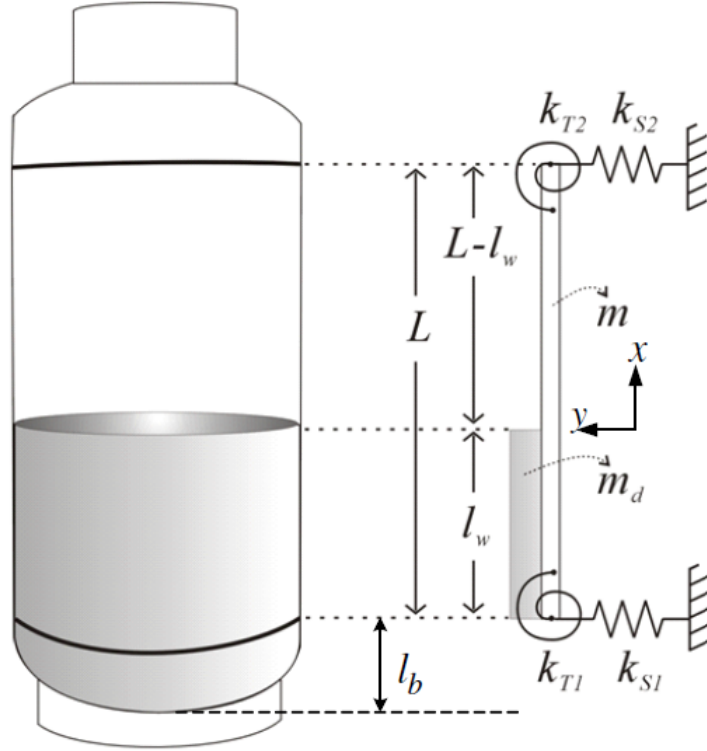
Figure 2.2: Mathematical model for a gas cylinder partially filed. Source:[2]

When a hammer is used to knock on the surface of the cylinder, the knock triggers a transverse vibration similar to a beam partially loaded with distributed mass. Since this similarity exists, the Euler-Bernoulli beam equation is applied.

As the cylinder is a simplification of a beam, it's necessary to define its boundary conditions. Because of the welded seams located on these extremities, this model considers two boundary conditions, one at the top and one at the bottom.

Assuming the mass per unit length of the beam to be m and the distributed mass per unit length m_d for the liquid part, the transverse vibration equation of the beam becomes:

$$
\begin{aligned}
EI\frac{d^4y_1}{dx^4} + (m + m_d)\frac{d^2y_1}{dt^2} &= 0 \quad for \quad -l_w \leq x < 0 \\
EI\frac{d^4y_2}{dx^4} + m\frac{d^2y_2}{dt^2} &= 0 \qquad\quad for \quad 0 < x < L - l_w
\end{aligned}
\tag{2.1}
$$

Where y_1 and y_2 are the transverse vibratory displacements of the beam.

The irregularities caused by the welding seams prevents an ideal clamped or pinned model because of the small displacements at the two boundaries (the one at the top and the one at the bottom).

The assumption of a linear and torsional spring to these boundaries solves this problem. If so, assuming a transverse vibration confined between two welding lines, the boundary conditions are:

- At $x = -l_w$

$$EI\frac{d^2y_1}{dx^2} = -k_{T1}\frac{dy_1(-l_w, t)}{dx}$$
$$EI\frac{d^3y_1(-l_w, t)}{dx^3} = -k_{S1}.y_1$$

(2.2)

- At $x = L - l_w$

$$EI\frac{d^2y_2}{dx^2} = -k_{T2}\frac{dy_2(L - l_w, t)}{dx}$$
$$EI\frac{d^3y_2(L - l_w, t)}{dx^3} = -k_{S2}.y_2$$

(2.3)

Where k_{S1} and k_{T1} are linear and torsional spring constants, respectively, for the lower part, while k_{S2} and k_{T2} are the same, but for the upper part.

The bottom of a gas cylinder usually has a circular steel plate which enables the stability of the cylinder when in contact with the ground. Because of this plate, it's possible to assume $k_{S1} > k_{S2}$ and $k_{T1} > k_{T2}$ since the lower part is more steady than the top part.

At the liquid level, the continuity and equilibrium conditions of this system are:

$$y_1(0, t) = y_2(0, t), \quad y_1'(0, t) = y_2'(0, t)$$
$$y_1''(0, t) = y_2''(0, t), \quad y_1'''(0, t) = y_2'''(0, t)$$

(2.4)

What makes possible to investigate the relationship of the normalized frequency ratio $fr = f/f0$ and the length ratio $lr = lw/L$[2].

2.3.3   The relation between models

Clamped-free boundary conditions

Chan et al[8] proposed this model to calculate the changes in the natural frequency of a cantilever tube, with a constant diameter, partially filled with liquid mercury.
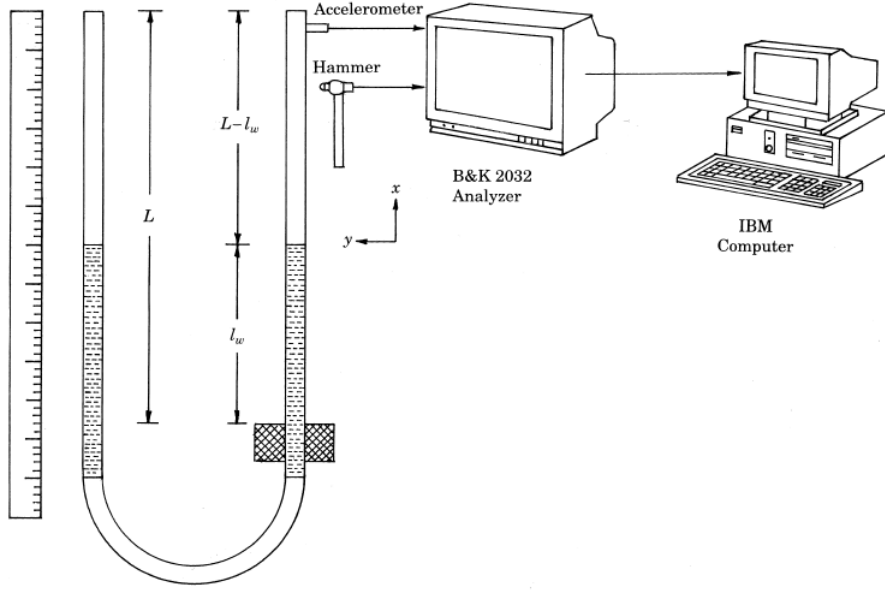
Figure 2.3: Clamped-free setup presented for calculating the natural frequency changes of a partially liquid filled cantiliver tube. Source:[8]

Figure 2.3 shows that the setup used by Chan et al[8] is a clamped-free model since the bottom of the cantilever was clamped, while the top was free. In this experiment, there was also transverse vibration generated by a hammer.

If we consider:

$$k_{S1} = k_{T1} \approx \infty \qquad k_{S2} = k_{T2} = 0 \tag{2.5}$$

We have the boundary conditions for the clamped-free model.

When, on equation 2.1, we replace the values of the linear and torsional springs by the values assumed in equation 2.5, with some mathematical manipulation[2], the boundary conditions at $x = -l_w$ and $x = L - l_w$ become the same as the one used on Chan's[8] work.

$$y_1(-l_w, t) = y_1'(-l_w, t) = y_2''(L - l_w, t) = y_2'''(L - l_w, t) = 0 \tag{2.6}$$

Pinned-pinned boundary condition

Chan et al[9] later extend their model to study a simply supported beam with an abrupt change of mass.
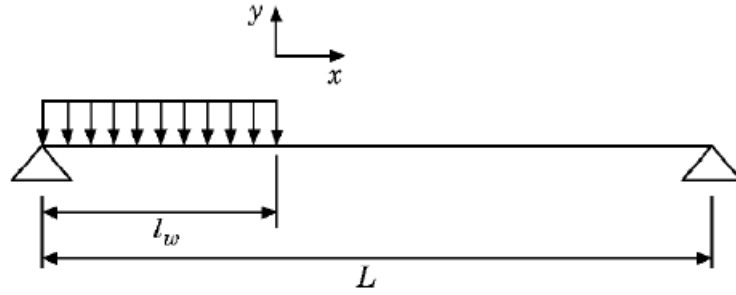
Figure 2.4: Pinned-pinned model proposed to study the vibrations of a simply supported beam partially loaded with distributed mass. Source:[9]

Being the boundary conditions:

$$k_{S1} = k_{S2} = \infty \qquad k_{T1} = k_{T2} = 0 \tag{2.7}$$

Just like for the clamped-free model, If we replace the values of equation 2.6 on equation 2.1 and with some mathematical manipulation[2] the boundary conditions for the pinned-pinned model at $x = -l_w$ and $x = L - l_w$ become the same as the one used on Chan's work.

$$y_1(-l_w, t) = y_1''(-l_w, t) = y_2(L - l_w, t) = y_2''(L - l_w, t) = 0 \tag{2.8}$$

Clamped-clamped boundary conditions

Jacobs et al[10] presented this method, which permitted the contactless measurement of liquid levels in thin opaque capillaries at high pressure. This method was also based on the mass dependence of the traverse resonance frequencies of a finite section of a tube.
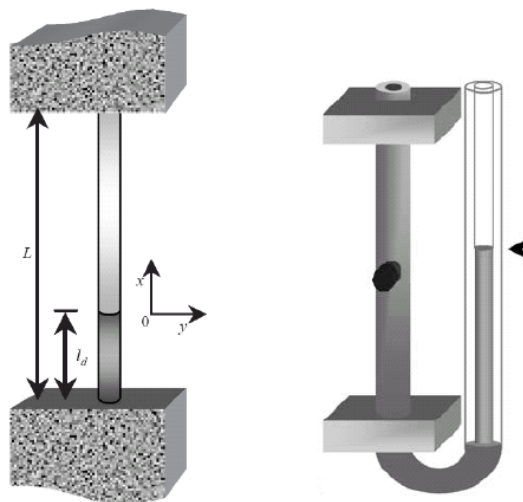
Figure 2.5: Clamped-clamped setup which permitted the contactless measurement of liquid levels in thin opaque capillaries at high pressure. Source:[10]

Being the boundary conditions:

$$k_{S1} = k_{S2} = k_{T1} = k_{T2} = \infty \tag{2.9}$$

Replacing the values of equation 2.9 on equation 2.1 and with some mathematical manipulation, the boundary conditions for the clamped-clamped model at $x = -l_w$ and $x = L - lw$ become the same as the one used on Jacobs et al[10] work.

$$y_1(-l_w, t) = y_1'(-l_w, t) = y_2(L - l_w, t) = y_2'(L - l_w, t) = 0 \tag{2.10}$$

New model vs old models

The model presented by Wu et al[2] is passive of manipulation through the control of the boundary conditions. By changing the values of the linear and torsional springs, the older models could be obtainable as seen previously. The continuity and equilibrium conditions support their model because they are the same as the one obtained previously by past works, even if the boundary conditions are different. This model is also the only that can be used when the spring and torsional constants (k_S, k_T) are not close to ∞ or 0[2].

2.3.4 Relation of the normalized frequency ratio and the length ratio

With the model presented by Wu et al[2], it's possible to simulate the curves of frequency versus length for the previous studies, by manipulation of the values of the linear and torsional springs to form the boundary conditions presented on equations 2.5, 2.7 and 2.9[2].

Figure 2.6 shows the frequency ratio $f_r = f/f_0$ and the length ratio $l_r = l_w/L$ of a clamped-free, pinned-pinned and clamped-clamped models.
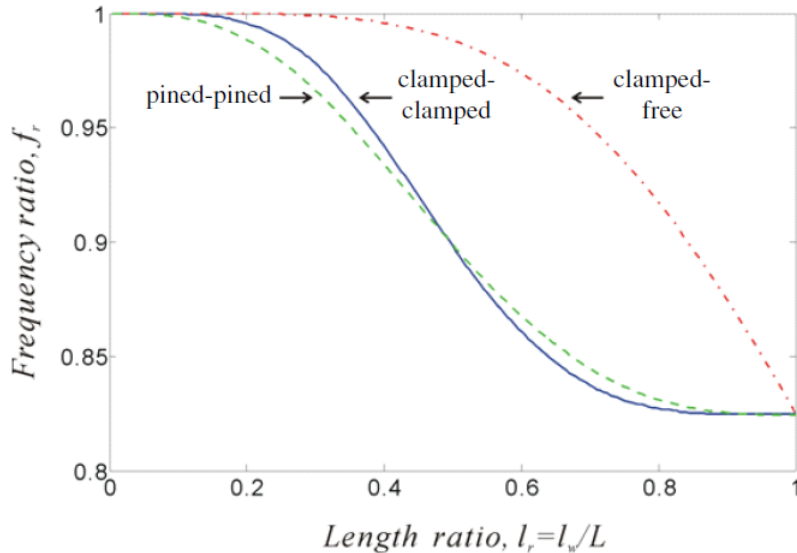
Figure 2.6: frequency ratio $f_r = f/f_0$ over length ratio $l_r = l_w/L$ of a clamped-free, pinned-pinned and clamped-clamped models. Source:[2]

For all three models, we can infer that:

- When the container is empty ($l_r -> 0$), the frequency ratio generated by the vibration is max ($f_r -> 1$).

- When the container is full ($l_r -> 1$), the frequency ratio is minimum ($f_r -> 0$).

The objective of Wu et al[2] was to recreate the same results obtained previously, but with their proposed model. With a setup based on a gas cylinder (Figure 2.2), a microphone to pick the transverse vibration and a computer to create its spectra and a graphical representation of the frequency ratio $f_r = f/f_0$ and the length ratio $l_r = l_w/L$, a similar result was obtained.
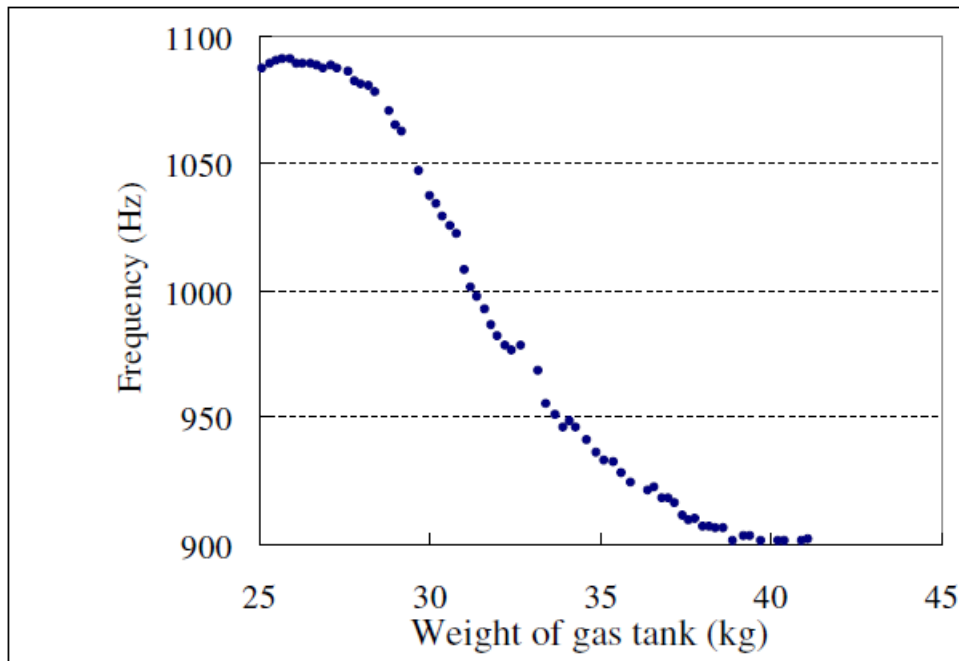
Figure 2.7: Variation of the frequency over the weight of the cylinder. Source:[2]

The plot of Figure 2.7 shows results similar to those presented in Figure 2.6 and proved that the weight, or the liquid level, is directly related to the frequency. This relation enables the estimation of the liquid level in a gas cylinder.

2.4   Impulse response of linear systems

2.4.1   Introduction

Until now, the focus has been on the explanation of the experiment with an emphasis on the mechanical part, but the digital signal processing of this is work is equally important and is where this work will focus. Next, follows a brief explanation of some important concepts that will help in the understanding of the work done on this master thesis in the subsequent Chapters.

2.4.2 Discrete-Time Signals

A discrete-time signal is a sequence of data where the elements of the sequence are denoted as samples and represented by $x(n)$, where n is the index associated with each sample and is an integer. These signals results of sampling a continuous-time signal $x_a(t)$ at a rate of $f_s = 1/T_s$. Equation 2.11 shows the relation between the sampled signal $x(n)$ and the continuous time signal $x_a(t)$[7].

$$x(n) = x_a(nT_s) \tag{2.11}$$

Some discrete signals are frequently used to represent more complicated signals, being the *Unit Sample* sequence one of them. This sequence is defined by:

$$\delta(n) = \begin{cases} 1 & ; & n = 0 \\ 0 & ; & \text{otherwise} \end{cases}$$

Which allows the decomposition of an arbitrary signal $x(n)$ into a sum of shifted unit samples.

$$x(n) = \sum_{k=-\infty}^{\infty} x(k)\delta(n-k) \tag{2.12}$$

2.4.3 Linear and Time-Invariance

Linearity

To measure the liquid level of a cylinder, it is first necessary to ascertain if the system is Linear and Time-Invariant (LTI). A linear system must respect a set of proprieties being the Linearity, and Time-Invariance considered of great importance for the analysis of these types of systems[7].

A linear system can be mathematically defined using the principle of superposition. For inputs $x_1(n)$ and $x_2(n)$, the output $y_1(n)$ and $y_2(n)$ are the response of a system H generated by the given input sequences. We have then:

$$y_1(n) = H[x_1(n)] \quad and \quad y_2(n) = H[x_2(n)] \tag{2.13}$$

Trough the superposition principle, a system H is linear if, for any input $x_1(n)$ and $x_2(n)$ when applied two constants a and b, results in:

$$H[ax_1(n) + bx_2(n)] = aH[x_1(n)] + bH[x_2(n)] \tag{2.14}$$

From equation 2.14, there are two conclusions to be taken:

- When there is a sum of two signals as an input of a linear system, the response of said system will be the sum of the two responses.

- When the input is multiplied by a constant its output is scaled by the same factor.

In order to show the importance of this propriety, it's possible to break down the input into a superposition of weighted and shifted unit samples, as seen previously in equation 2.12. The output is then:

$$
\begin{aligned}
y(n) &= \sum_{k=-\infty}^{\infty} x(k)H[\delta(n-k)] \\
&= \sum_{k=-\infty}^{\infty} x(k)h_k(n)
\end{aligned}
\tag{2.15}
$$

Trough equation 2.15 we conclude that if $h_k(n)$ is known, it's possible to specify a linear system completely since $h_k(n)$ is the response of the system to the impulse $\delta(n-k)$.

Time-Invariance

In a Time-Invariant system, whenever the input experiences a shift of n_0 samples, the output will also experience the same shift of n_0 samples. That is to say, in a system with input $x(n)$ and response $y(n)$, every time that happens a shift in the input by n_0 samples, namely $x(n-n_0)$, the response of the system will also be $y(n-n_0)$, meaning that the system does not change over time[7].

LTI

When the last two properties manifest in a system, the system is designated Linear and Time-Invariant (LTI). In a Time-Invariant system, if the response of an impulse $\delta(n)$ is $h(n) = H[\delta(n)]$, then the response of $\delta(n-k)$ is $h(n-k)$. If we take equation 2.15 and use it for an LTI system it becomes:

$$
y(n) = \sum_{k=-\infty}^{\infty} x(k)h(n-k) = \sum_{k=-\infty}^{\infty} x(n-k)h(k)
\tag{2.16}
$$

This equation is designated the convolution sum and can be simplified in:

$$
y(n) = x(n) * h(n)
\tag{2.17}
$$

We now have a tool that helps in assessing the response of an LTI system for any input $x(n)$. This response known as $h(n)$ is referred to as the impulse response of the system[7].

2.4.4   Discrete-Time Fourier Transform

Besides the impulse response of a system, the Fourier transform is also one of the possible mathematical tools used in the analysis of an LTI system[14].

The Fourier transform allows decomposing a signal into a sum of sinusoids or a sum of complex exponential. This decomposition changes the domain of the signal, now represented in the frequency domain.

The decomposition of signals is important in the analysis of LTI systems. When a sinusoid is used as an input for an LTI system, its response is a sinusoid with different amplitude and phase, but with the same frequency as the input. Even if the input is a sum of sinusoids,

thanks to the Linearity propriety, the output will also be a sum of sinusoids, but with different amplitude and phase.

To investigate discrete signals is used the Discrete-Time Fourier Transform (DTFT). The DTFT of a signal $x(n)$ is a complex-valued function of w (discrete frequency variable) given by[7]:

$$X(e^{jw}) = \sum_{n=-\infty}^{\infty} x(n)e^{-jnw} \tag{2.18}$$

Where the sum of $x(n)$ converges to equation 2.19, that is the condition that defines the DTFT of a signal.

$$\sum_{n=-\infty}^{\infty} |x(n)| < \infty \tag{2.19}$$

To transform a signal from time domain to frequency domain, a set of properties are followed, being the most important presented on table 2.1.

Table 2.1: Properties of the DTFT

Property	Sequence	Transform
	$x(n)$	$X(e^{jw})$
Delay	$x(n-n_0)$	$e^{-jwn_0}X(e^{jw})$
Modulation	$e^{jw_0 n}x(n)$	$X(e^{j(w-w_0)})$
Conjugation	$x^*(n)$	$X^*(e^{-jw})$
Time reversal	$x(-n)$	$X(e^{-jw})$
Convolution	$x(n)*y(n)$	$X(e^{jw})Y(e^{jw})$
Multiplication	$x(n)y(n)$	$\frac{1}{2\pi}\int_{-\pi}^{\pi} X(e^{j\theta})Y(e^{j(w-\theta)})d\theta$

One of the most important DTFT belongs to the unit sample. The DTFT of a unit sample defines how a complex exponential is changed in amplitude and phase by a generic system H. Because of that, equation 2.20 is called the frequency response of a filter.

$$H(e^{jw}) = \sum_{n=-\infty}^{\infty} h(n)e^{-jnw} \tag{2.20}$$

2.4.5 Impulse response of a gas cylinder

Ideally, an impulse is a signal composed of all zeros, except in a single moment, where its value is different from zero[13]. As seen previously, the impulse response also helps to assess the response of an LTI system.

To measure the liquid level inside a gas cylinder, Wu et al[2] used a hammer to knock on the cylinder and recorded its traverse vibration. The knock of a hammer is a good approximation to an ideal impulse, able to excite the needed frequencies.

Through equation 2.17, it's possible to observe that the output of a system depends on its input $x(n)$ and its response $h(n)$. When the input signal is an impulse, the output becomes

the system response.

$$y(n) = h(n) \qquad (2.21)$$

Since the system response of the cylinder is known, the next step is the application of the Fourier transform to study the frequency response of the system.
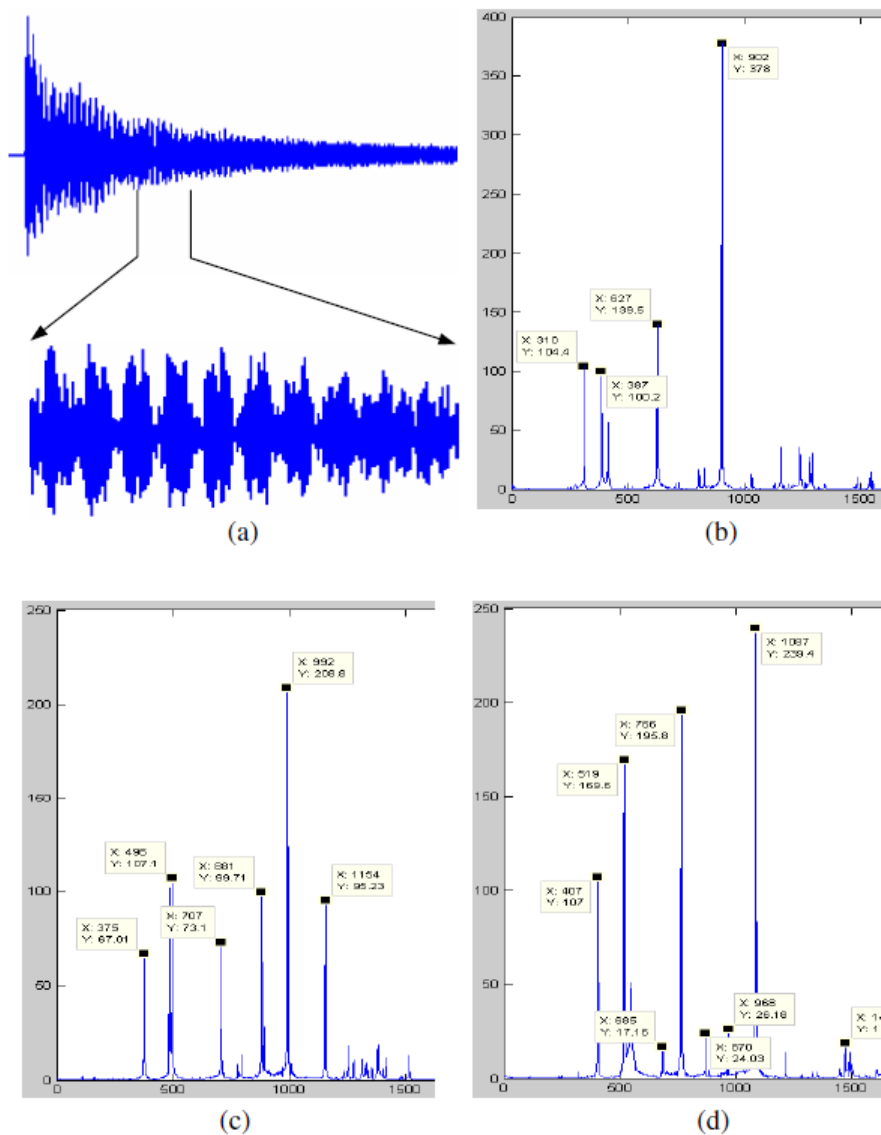
Figure 2.8: (a) - The impulse response and the section used to obtain the frequency components, (b) - Frequency components of an almost full cylinder, (c) - Frequency components of a half full cylinder, (d) - Frequency components of an empty cylinder Source:[2]

Figure 2.8 shows the frequency response of the system to 3 different cylinders with different

14

volume of liquid, where the frequency with a higher magnitude, is the frequency related to the traverse vibration. This frequency can also be related to the weight of the gas inside the cylinder as seen previously on Figure 2.7.

2.5 Indirect measurement techniques

2.5.1 Introduction

With the method proposed by Wu et al[2], it's possible to measure the liquid level of a gas cylinder relating the frequency with weight. The problem with this method is the use of the hammer. In a laboratory environment, it's possible to use a hammer to knock on a gas cylinder but in a familiar environment, a user wouldn't want the hassle of knocking in the cylinder to check the level of gas.

A possible upgrade for the proposed method is the substitution of the hammer with a small piezoelectric speaker where a convenient signal is applied. One possible signal is the chirp signal, that allows to obtain the impulse response of the observed system using cross-correlation.

2.5.2 Linear Chirp

A Chirp is a signal in which its frequency varies with time. The range of frequency variation is defined by f_0 and f_1, which enables the study of the frequency response of a system in this defined range of the spectra[15].
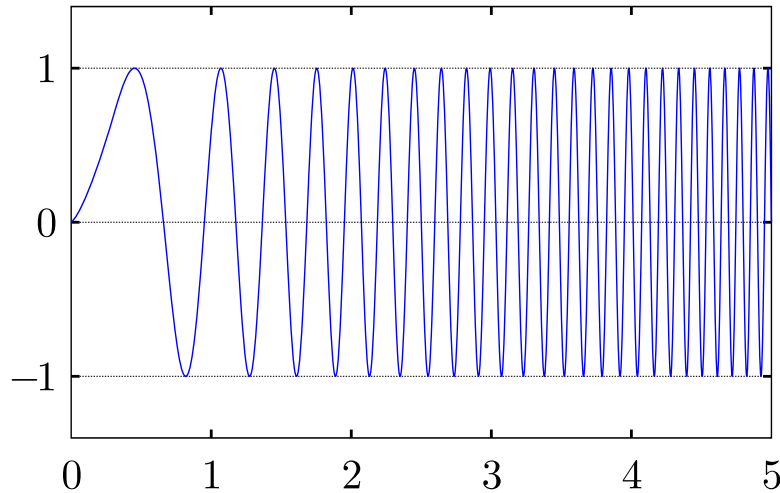
Figure 2.9: Waveform of a linear chirp. Source:[16]

The equation of a linear chirp is obtained through the equation of the sinusoid but with some considerations. Consider equation 2.22, the equation of a sinusoid:

$$x(t) = A\cos(w_0 t + \theta) \tag{2.22}$$

15

The argument of the cosine is the instantaneous phase, represented by ϕ.

$$x(t) = A\cos(\phi(t)) \tag{2.23}$$

Is possible to obtain the instantaneous angular frequency by the derivative of the instantaneous phase which is the instantaneous slope of ϕ.

$$w_i(t) = \frac{d}{dt}\phi(t) \quad (rad/s) \tag{2.24}$$

Since equation 2.24 is the instantaneous angular frequency, its units will be in rad/s. The SI unit of frequency is Hertz (Hz). By dividing equation 2.24 by 2π, we now have the instantaneous frequency.

$$f_i(t) = \frac{1}{2\pi}\frac{d}{dt}\phi(t) \quad (Hz) \tag{2.25}$$

If ϕ is a quadratic signal as shown on equation 2.26, its derivative is given by equation 2.27.

$$\phi(t) = 2\pi\mu t^2 + 2\pi f_0 t + \theta \tag{2.26}$$

$$f_i(t) = 2\mu t + f_0 \tag{2.27}$$

The frequency variation produced by equation 2.26 is known as frequency modulation. These signals are known as chirps because equation 2.27 produces a sound that resembles the chirp of a bird.

Knowing that a chirp is a frequency sweep between two frequencies, its spectra vary linearly with time. Since the variation is linear, a slope is created. By calculating this slope, it's possible to obtain the value for the instantaneous frequency, which is now given by equation 2.28.

$$f_i(t) = \frac{f_1 - f_0}{T}t + f_0 \tag{2.28}$$

Finally, the instantaneous phase ϕ is the integral of equation 2.24.

$$\phi(t) = \int_0^t w_i(u) \quad du \tag{2.29}$$

Through equations 2.24 and 2.25, equation 2.29 simplifies to:

$$\phi(t) = \int_0^t 2\pi f_i(u) \quad du \tag{2.30}$$

In conclusion, is possible to define a time-domain chirp signal by equation 2.31.

$$x(t) = A\cos\left(2\pi\left(\frac{1}{2}\frac{f_1 - f_0}{T}t^2 + f_0 t\right)\right) \tag{2.31}$$

On the discrete domain, equation 2.31 becomes:

$$x(n) = A\cos\left(2\pi\left(\frac{1}{2}\frac{f_1 - f_0}{T}\left(\frac{n}{f_s}\right)^2 + f_0\frac{n}{fs}\right)\right) \tag{2.32}$$

The reason the input signal $x(n)$ is a linear chirp, is because of its autocorrelation characteristics.

2.5.3 Correlation technique

In signal processing is usually necessary to compare two signals and understand the similarities between them. The correlation is a mathematical process that allows this comparison[17].

By considering two random data sequences, when the sum of the product between these signals tends to a small number, it means that these signals are correlated. The sum tends to a small value, because of the probability of a positive or negative number being the same, which cancels the pair of products when summed.

The cross-correlation between two data sequences $x(n)$ and $y(n)$, each with N samples, is given by equation 2.33.

$$R_{xy} = \sum_{n=0}^{N-1} x(n)y(n) \tag{2.33}$$

Since the result of equation 2.33 depends on the number of sampling points, is necessary to normalize the result, dividing by the total number of samples N. Equation 2.33 becomes equation 2.34 and is now regarded as the averaging sum of products.

$$R_{xy} = \frac{1}{N} \sum_{n=0}^{N-1} x(n)y(n) \tag{2.34}$$

The problem with equation 2.34 is the non consideration of lag. If two signals are 100% correlated but one of them is out of phase with the other, equation 2.34 may indicate that the signals are not correlated. Figure 2.10 illustrate this problem.
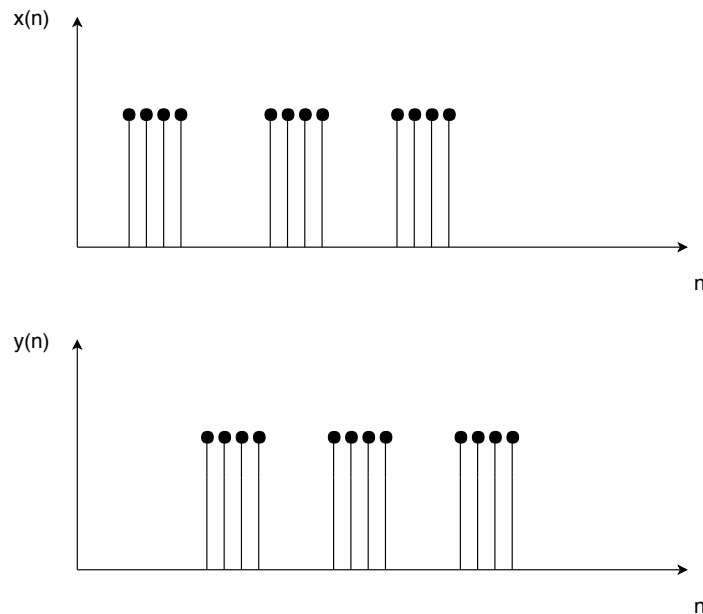
Figure 2.10: Waveforms with zero correlation because of the phase difference.

To guarantee that both signals have the same phase it's necessary to shift one of the signals, maintaining the other still. This shift is usually known as lag.

As $x(n)$ and $y(n)$ are the same signal but with a different phase, by shifting $y(n)$ to the left, or $x(n)$ to the right, the phase of the two signals becomes the same. To do that is necessary to change the argument of $x(n)$ or $y(n)$ in equation 2.34, that becomes:

$$R_{xy}(l) = \frac{1}{N} \sum_{n=0}^{N-1} x(n)y(n+l) \tag{2.35}$$

Which is the same as:

$$R_{yx}(-l) = \frac{1}{N} \sum_{n=0}^{N-1} y(n)x(n-l) \tag{2.36}$$

In practice, the phase of x and y is unknown. To calculate the cross-correlation between two signals, it's necessary to use different values of lag to discover the largest value of the correlation between them. This value shows to which value of lag, signals x and y have a higher correlation.

When x and y are the same $(x(n) = y(n))$, The signal is cross-correlated with itself. This process is known as autocorrelation and is given by equation 2.37.

$$R_{xx}(l) = \frac{1}{N} \sum_{n=0}^{N-1} x(n)x(n+l) \tag{2.37}$$

One of the great advantages of the autocorrelation is that it allows the calculation of the energy of a signal.

$$E = R_{xx}(0) = \frac{1}{N} \sum_{n=0}^{N-1} x^2(n) \tag{2.38}$$

For a random signal like, for example, white noise, it's possible to see through Figure 2.11 that the autocorrelation has its peak at zero lag and decreases to a value next to zero for greater values of lag.
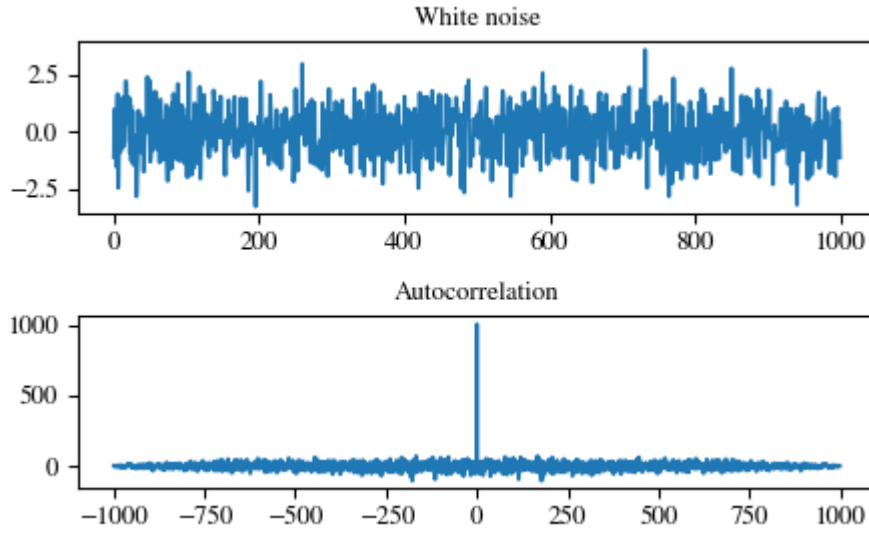
Figure 2.11: Autocorrelation of a white noise signal. Souce:[18]

2.5.4   Finding the impulse response of a system using correlation

In an LTI system, when the input signal has an autocorrelation that is approximately an impulse, the correlation between the input signal and the output gives us the response of the system[19].
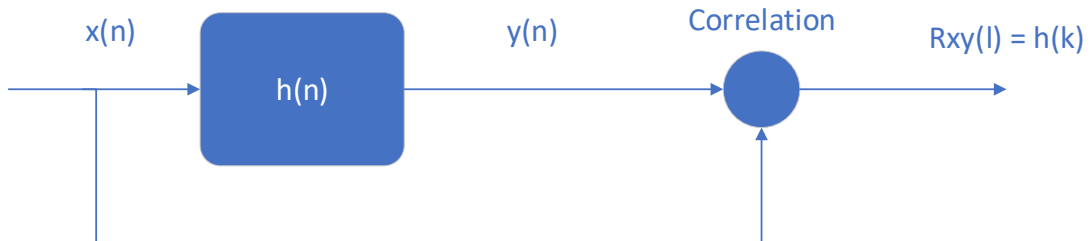
Figure 2.12: Block diagram of the correlation method

The cross-correlation between two data sequences, each with N samples, is given by equation 2.35, where:

$$
\begin{aligned}
y(n+l) &= \sum_{k=0}^{N} x(k)h(n+l-k) \\
&= \sum_{k=0}^{N} x(n+l-k)h(k)
\end{aligned}
\tag{2.39}
$$

Equation 2.35 now becomes:

$$R_{xy}(l) = \frac{1}{N} \sum_{n=0}^{N-1} x(n) \left(\sum_{k=0}^{N} x(n+l-k)h(k) \right)$$
$$= \frac{1}{N} \sum_{k=0}^{N} h(k) \left(\sum_{n=0}^{N-1} x(n)x(n+l-k) \right) \quad (2.40)$$
$$= \frac{1}{N} \sum_{k=0}^{N} h(k)R_{xx}(l-k)$$

Since the autocorrelation of the input signal is considered an approximation of an impulse, the following equality of equation 2.41 is valid.

$$R_{xx}(l-k) = \delta(l-k) \quad (2.41)$$

The unit sample now depends on the values of l and k becoming:

$$\delta(l-k) = \begin{cases} 1 & ; \quad l = k \\ 0 & ; \quad l \neq k \end{cases}$$

Is easy to perceive trough equation 2.42 that if the input signal is an impulse, the output is the response of the system.

$$R_{xy}(l) = \frac{1}{N} \sum_{k=0}^{N} h(k)R_{xx}(l-k)$$
$$= h(k) \quad (2.42)$$

The linear chirp is one of the signals where its autocorrelation is approximately an impulse, being this the reason of why it was selected.

Chapter 3

Liquid level measurement by direct impulse response

3.1 Introduction

As seen previously, a good approach to detect the liquid level in an LPG cylinder without the need to install a transmitter or a receiver inside the tank is the impulse response. Is easy to reproduce an approximation of an impulse and the impulse response of an LTI system shows the behavior of the system, making it a method of choice.

Since the knock of a hammer qualifies as an impulse because there's energy transferred to the cylinder only in the moment of the impact, with its usage is possible to discover the behavior of the cylinder, but first is necessary to build an experimental setup and confirm if the cylinder is really Linear and Time-Invariant.

If the system is Linear and Time-Invariant, is possible to apply the properties described previously, in order to obtain its impulse and frequency responses.

3.2 Experimental setup

The experimental setup consists of a cylinder, a microphone to record the impulse response, a soundboard to acquire the recorded data and communicate with the computer, a computer to process the recorded data, and the respective cables. Figures 3.1 and 3.2 show the assembled setup and the equivalent block diagram.

The input signal is the impulse that the hammer creates in the moment of the knock which generates the response of the system $H(s)$. This response denoted as $Y(s)$ is filtered by a Low Pass Filter (LPF) and an Analog to Digital Converter (ADC) from a soundboard. The soundboard converts the analog signal into a digital signal to be processed by a computer.

Figure 3.1: Experimental setup used to record the impulse response.
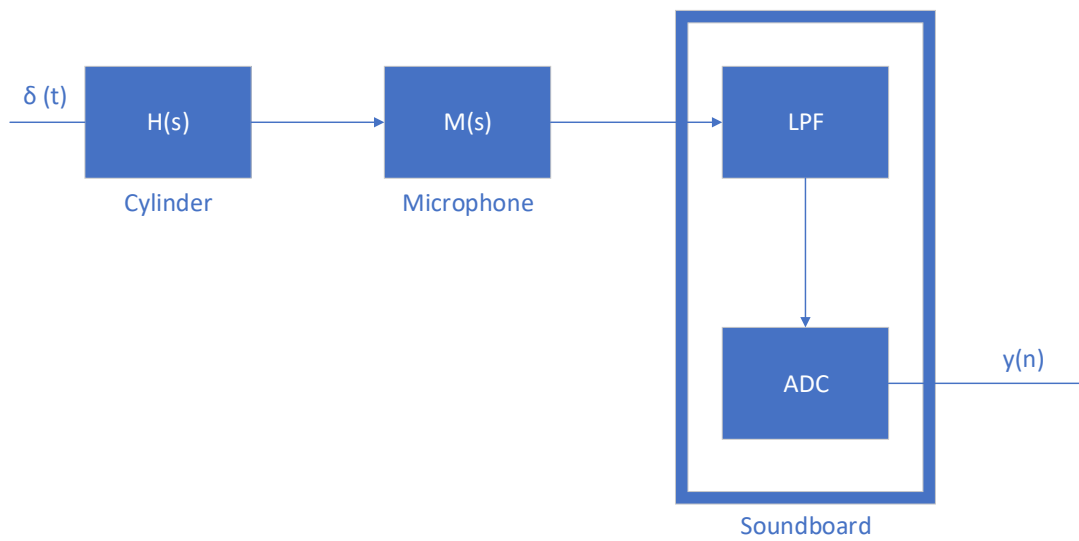
Figure 3.2: Block diagram of the experimental setup.

Since it's important to document the hardware and software used on this work, a brief explanation about them will be provided for a better understanding of the experimental setup.

3.2.1 Hardware and Software

Hardware

The two fundamental pieces of hardware necessary for the realization of this work are the soundboard and the microphone.

The soundboard is a Roland $FA - 66$ (discontinued at the time of writing). This soundboard has 2 XLR/TRS input jacks that allow the connection of several types of equipment. These inputs have high gain microphone preamps and phantom power $(48V)$, allowing the connection of condenser microphones. A headphone jack output is responsible for output the mixed sound inputted by the input jacks and the sound outputted by the computer. The output volume, as well as the input sensitivity, can be controlled. This soundboard has a $24bit/192\,kHz$ audio quality and a $FireWire$ audio interface dedicated only for audio/video giving a low latency performance. It should be noted that a motherboard compatible with $FireWire$ is necessary[20].

Figures 3.3 and 3.4 show the front connections and the back connections of the soundboard used in this work.

Figure 3.3: Front connections of the soundboard.

Figure 3.4: Rear connections of the soundboard.

The microphone is a behringer ECM8000.

Figure 3.5: Behringer ECM8000 used.

This microphone has a precise electret condenser powered by $+15V$ to $+48V$ of phantom power and an ultra-low noise Field-Effect Transistor (FET) that eliminates low-frequency distortion. It has an ultra-linear frequency response with a response range from $15Hz$ to

$20kHz$ and an omnidirectional pattern with a sensitivity of $-60dB$. The connector, gold-plated XLR, allows higher signal integrity[21].
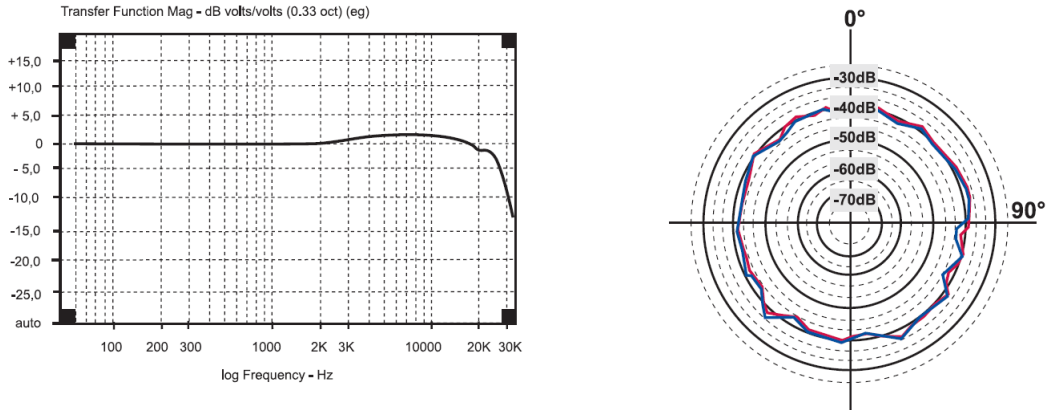
Figure 3.6: Frequency response and sensibility of the ECM8000. Source:[21]

Software

The only software used in this work was the MATLAB program. MATLAB stands for MATrix LABoratory and is a programming platform that allows development of algorithms, analysis of data and creation of models. During the execution of this work, this program was used for simulations, plots and signal and data processing, possible by its signal processing toolbox.

3.3 Linear system measurement

To confirm the linearity and time invariance properties of the cylinder is necessary to add a contact speaker to the setup presented on Figure 3.1 (Refer to Section 4.2 from Chapter 4 for a better understanding of the experimental setup). As seen previously, when a sinusoid is used as an input for an LTI system, its response is a sinusoid with different amplitude and phase but with the same frequency as the input[14]. The speaker is responsible for the reproduction of these sinusoidal waves.

Recalling the block diagram of a discrete system represented in Figure 2.1, by applying a sinusoidal wave as the input signal $x(n)$ and verifying the frequency response of the output $y(n)$, is possible to ascertain if the cylinder is an LTI system.

In practice, two sinusoidal waves were generated by MATLAB, with frequencies $f_1 = 1100Hz$ and $f_2 = 1500Hz$. The frequency value is arbitrary. The digital signal produced by MATLAB is converted to analog through the DAC of the soundboard and is reproduced by a contact speaker connected through the output jack. The sound reproduced by the speaker is recorded by the adjacent microphone, converted to digital through the ADC of the soundboard and processed again by MATLAB. Figures 3.7 and 3.8 shows the frequency response of the two sinusoids.
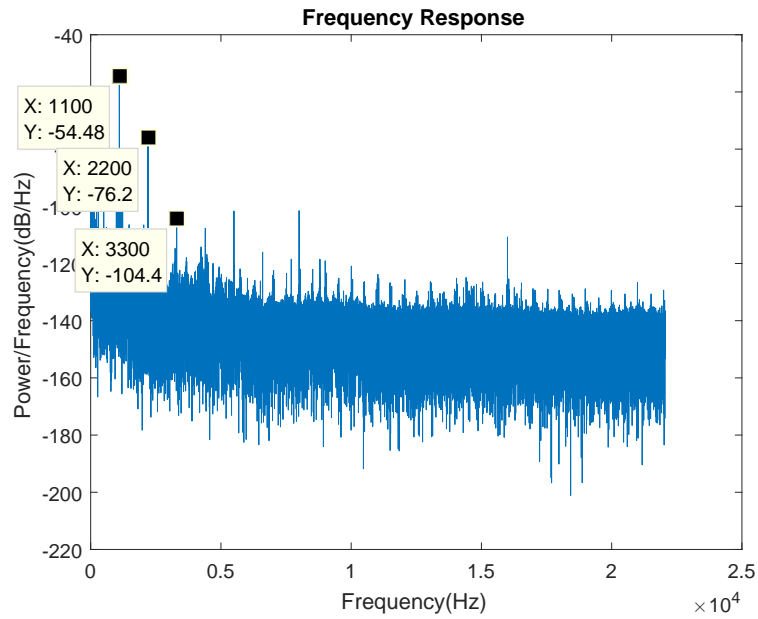
Figure 3.7: Frequency response of the cylinder when the input is a sinusoid with frequency of 1100 Hz.
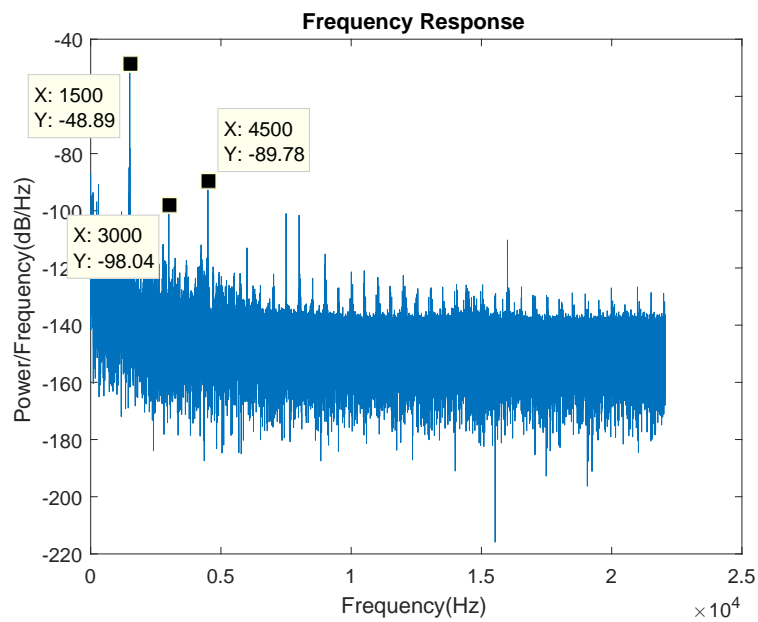
Figure 3.8: Frequency response of the cylinder when the input is a sinusoid with frequency of 1500 Hz.

It is possible to confirm the linearity of the cylinder since Figures 3.7 and 3.8 shows that the output frequency is the same as the input, being also possible to see the harmonic distortion that appear on the multiples of the input frequency.

Since the tests were repeated several times and the obtained results were always the same for the the frequencies of the sinusoidal wave and its harmonics, it will be considered that the cylinder is time-invariant.

Being the cylinder linear and considered LTI, it is possible to proceed to next step that is the impulse response measurement with a hammer.

3.4 Detection with a hammer

3.4.1 Impulse response

To measure the impulse response of the cylinder is necessary to generate an impulse. Since the knock of a hammer qualifies as an impulse, the hammer is responsible to create the impulse response of the cylinder. With the impulse response, it's also possible to calculate the frequency response. The frequency response will be responsible for the assessment of the liquid level of the gas inside the cylinder.

One of the steps from the work proposed by Wu et al[2] consisted on the release of gas until the cylinder was empty. To avoid the careless release of gas, since it is necessary to have a controlled environment, three cylinders with different levels of gas were used. One full, weighing up to $9Kg$ of net weight, the second only had half of its content while the last one was empty. The three cylinders give us the range that the frequency varies from full to empty.

Figure 3.9: From left to right: full cylinder, half and empty.

A knock was then applied to every cylinder. The impulse response of the three cylinders is shown on Figures 3.10, 3.11, 3.12.
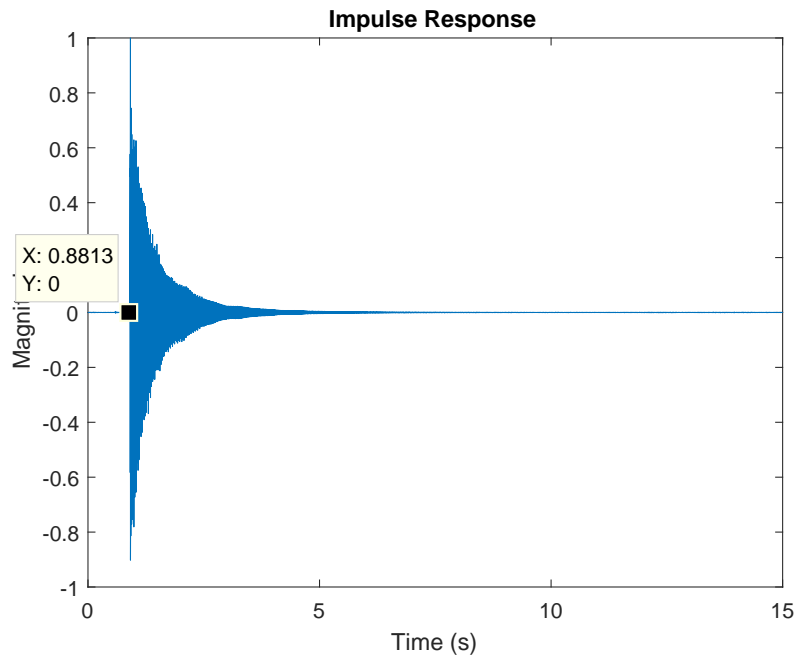
Figure 3.10: Impulse response of full cylinder.
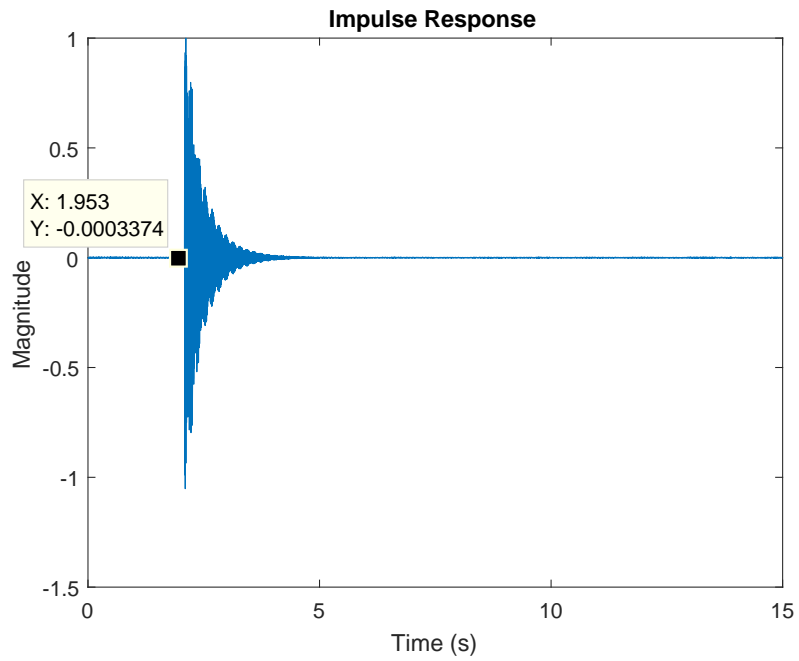
Figure 3.11: Impulse response of half full cylinder.
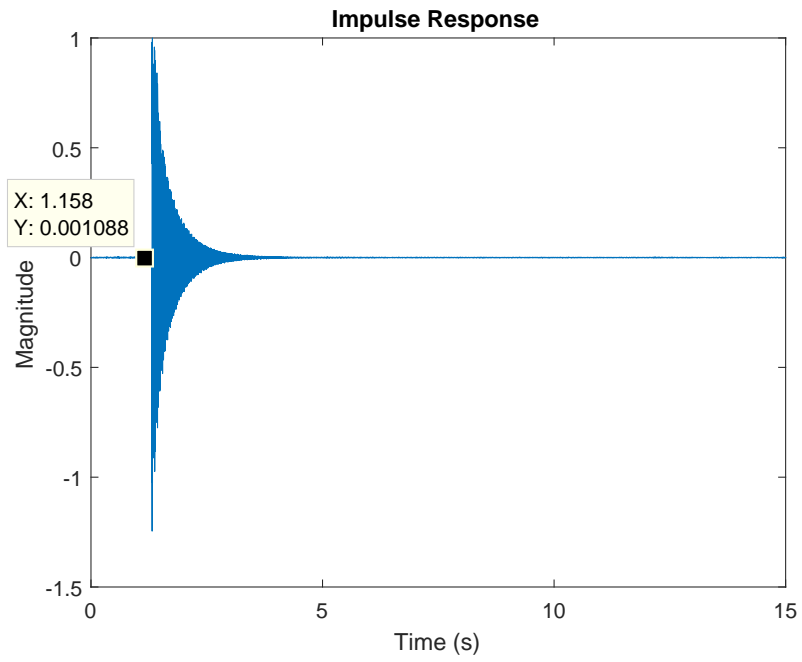
Figure 3.12: Impulse response of empty cylinder.

Figure 3.13: Spectrogram of full cylinder.

Figure 3.14: Spectrogram half full cylinder.
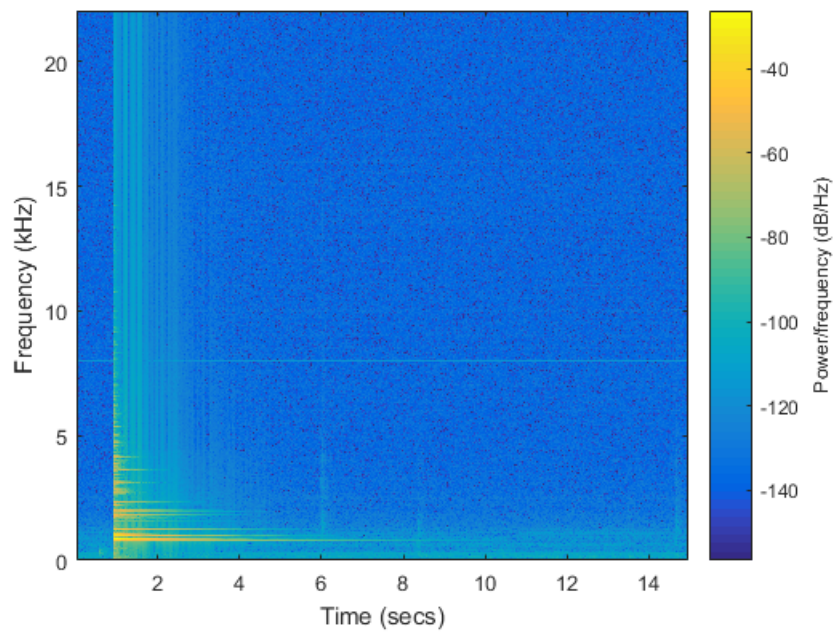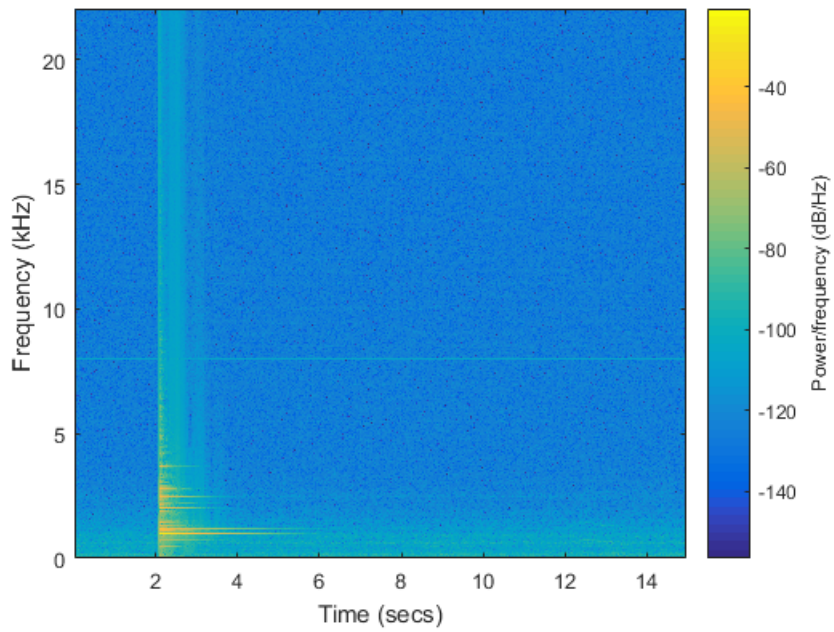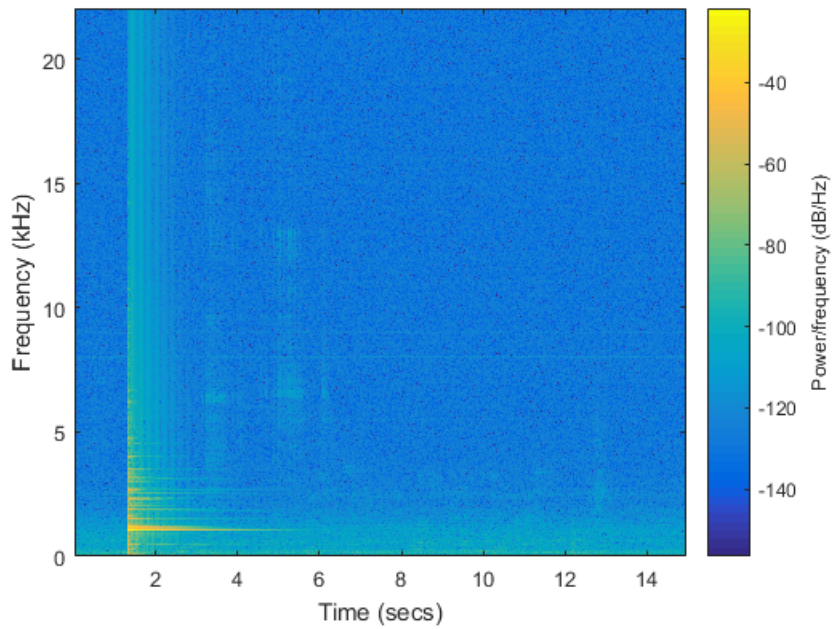

Figure 3.15: Spectrogram of empty cylinder.

Since the knock is manual and not controlled by a machine, it's possible to observe that the impulse has a lag from the start of the recording. The duration of the recorded signal chosen was 15 seconds, to guarantee the recording of the spectral components with a higher

Power Spectrum Density (PSD) since, in the moment of the knock, there is a manifestation of numerous frequencies. A further explanation about the PSD is shown on section 3.4.2. Figures 3.13, 3.14 and 3.15 show the spectrogram of the recorded signals.

The spectrogram of a signal allows the observation of the frequency content over time in the system. For each cylinder, during the initial seconds, many frequencies have a high spectral power that fades away as time goes by. The frequency with a higher spectral density over an extended period of time is the frequency where the impulse resonates more giving us a landmark to measure the liquid level of the cylinder.

3.4.2 Frequency response

PSD estimation and Welch's Method

Since the impulse is not a predetermined signal and is generated only at the moment of the knock, it is not possible to use the correlation of two signals to estimate the frequency response of the system, because the recorded signal is already the impulse response of the cylinder. Thus, to measure the frequency response of an impulse, it was used the Welch's method of PSD estimation.

The PSD is defined as the DTFT of the autocorrelation function as shown in equation 3.1[22].

$$P_{xx}(f) = T \sum_{m=-\infty}^{\infty} R_{xx}[m]e^{jwmT} \tag{3.1}$$

Equation 3.1 states that an infinite number of samples is necessary to compute with precision the Power Spectrum Density of a signal. Since, in practice, all signals have a finite length, some methods of PSD were developed, being the Welch's method one of them.

There are two categories of spectrum estimation, parametric and nonparametric. Since the parametric methods consume time and effort to create a model while the nonparametric method has the advantage of implementation through the Fast Fourier Transform (FFT), in this work, the explanation about parametric methods will be disregarded.

The first method presented to estimate the PSD is the periodogram. The problem with this method is that successive realizations yield unstable estimates, except for a larger number of data samples. By dividing a discrete signal, with a finite number of samples, in smaller segments (windowing) and averaging their spectra, the results become more stable and accurate. This is the Bartlett method. Welchs method reduces further the variance of the PSD when compared with Bartletts method, at the expense of a decrease in spectral resolution. This is achieved by windowing the segments and overlapping them. When the samples overlap, the number of segments to average increases, decreasing the variance of the PSD. The type of window chosen is equally important since it reduces the spectral leakage[17].

Figures 3.16 and 3.17 shows the resulting PSD estimate from the recorded signal with windowed data segments (Hann window) and without windowed data segments (rectangular window).
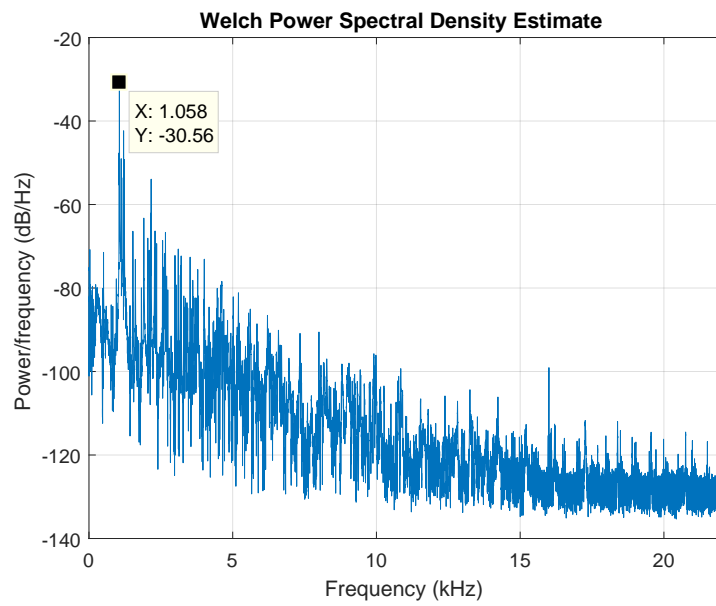
Figure 3.16: Welch Power Spectral Density estimate for a signal without windowed data segments (The length of the data segment is equal to the length of the signal).
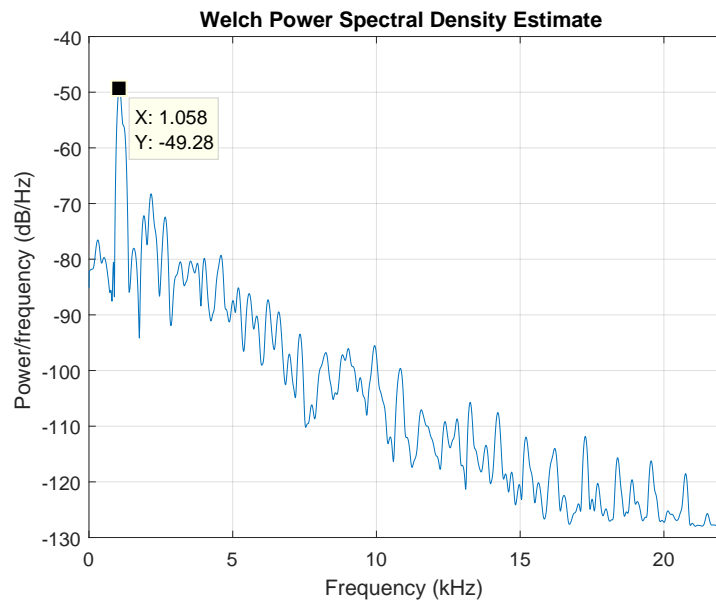
Figure 3.17: Welch Power Spectral Density estimate for a signal with windowed data segments (Hann window with data segments of 512 samples).

When there is an increase in the number of samples in a data segment, there are fewer data segments averaged together, increasing the frequency resolution but decreasing the smoothness. It's possible to observe on Figures 3.16 and 3.17 that the signal with windowed data segments has a higher smoothness in the spectral estimate in comparison with the signal without windowed data segments because of the higher number of data segments that are averaged together.

In conclusion, the Welch's method provide a more reliable method of Power Spectrum Density estimation when compared to its predecessor, thanks to the windowing of data and the overlapping of samples.

Frequency Response of the cylinder

With the impulse response measured, it's possible to measure the frequency response of the cylinder. With the frequency response of the cylinder, is possible to distinguish the liquid level through the frequency with the highest magnitude. To measure the frequency response of the cylinder, it was used the Welch's method of PSD estimation.

The Welch's method was applied to all the signal with an window of 512 samples and an overlapping of samples of 50%.
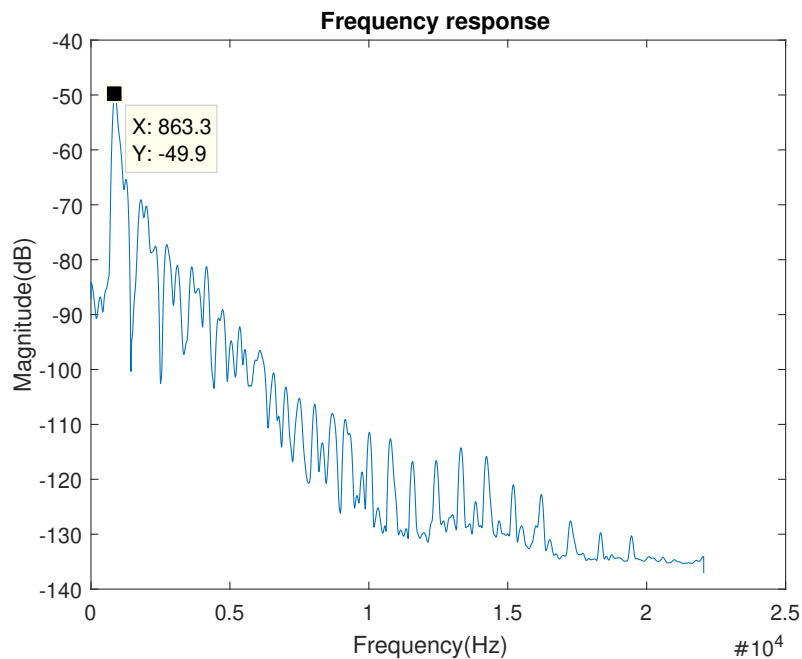
Figure 3.18: Frequency response of full cylinder.
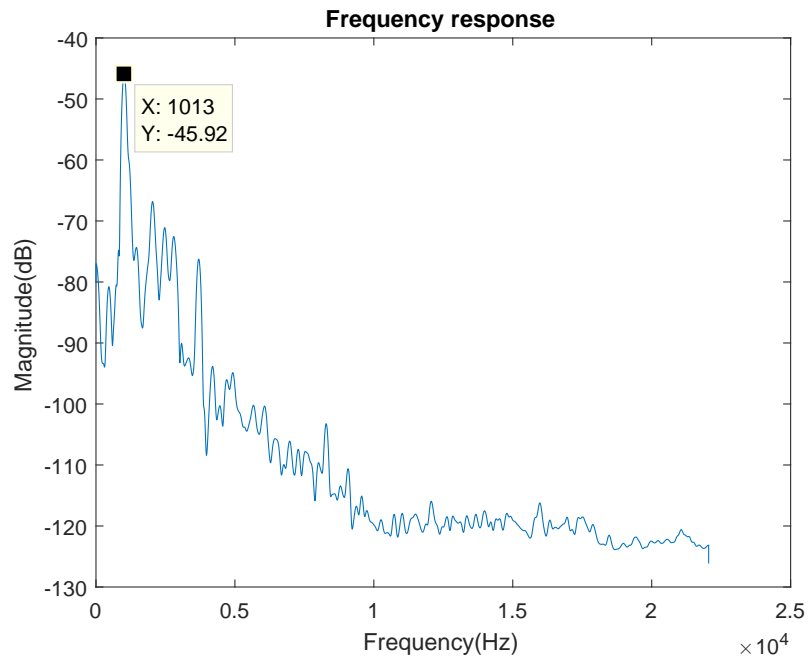
Figure 3.19: Frequency response of half full cylinder.
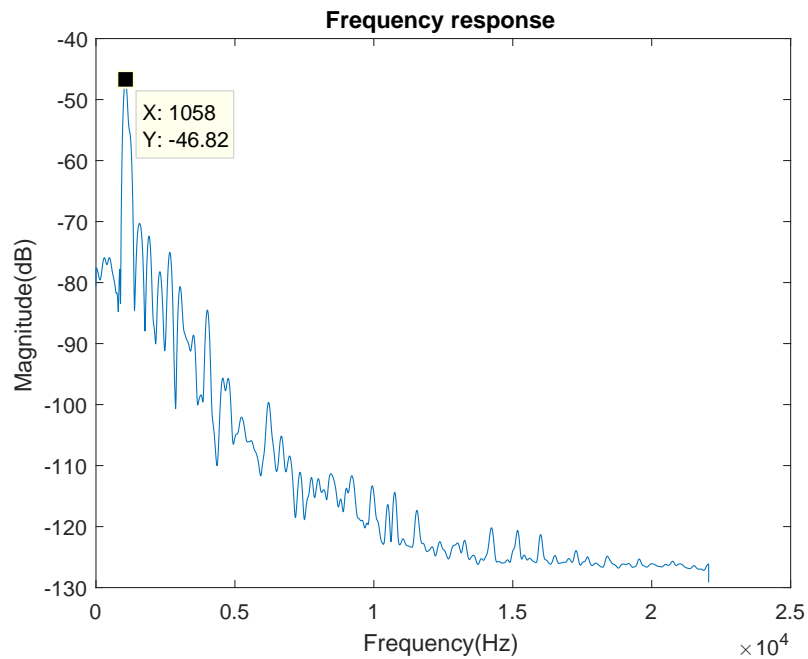
Figure 3.20: Frequency response of empty cylinder.

Figures 3.18, 3.19 and 3.20 show the frequency response of the three cylinders. The frequency with the higher magnitude for each cylinder is, respectively, $863.3Hz$, $1013Hz$, and $1058Hz$.

Table 3.1: Map of the weight of the gas cylinder with its corresponding frequency (direct method)

Weight	Frequency
$Full$	$863.3Hz$
$Half - full$	$1013Hz$
$Empty$	$1058Hz$

By observation of the frequency response plots of the three cylinders, is possible to create a map between the frequency and the weight ranging to $860Hz$ to $1060Hz$ approximately. The empty cylinder will always have a higher frequency while the full cylinder has a lower frequency.
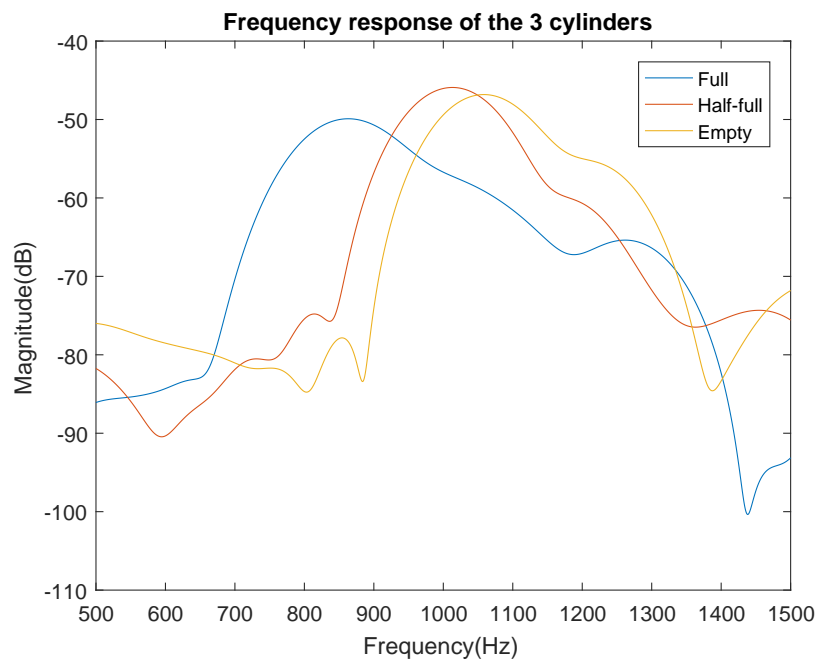
Figure 3.21: Frequency response of empty cylinder.

In practice, it's possible to discover the weight of a cylinder by applying an impulse and calculating it's frequency response. Although this is true in a laboratory environment, it's not practical to a distributor or a user, to knock with a hammer in the cylinder when needs to measure if the cylinder is full or empty. In the next chapter, a method to measure the impulse and frequency response is proposed in order to substitute the use of a hammer to a loudspeaker and perform the correlation.

Chapter 4

Liquid level measurement by indirect impulse response

4.1   Introduction

In the last chapter, the impulse response, and the frequency response were measured and a model to map the resultant frequency with the weight of the cylinder was defined. The problem with this method consists of the use of a hammer, which is impractical outside of a laboratory environment.

One solution proposed is the substitution of the hammer for a speaker applying a chirp signal. The chirp has an autocorrelation that is approximately an impulse allowing the measurement of the cylinder impulse response.

The big difference between the hammer and the chirp is that the hammer is approximately an impulse that is directly applied to the cylinder, being this method considered a direct method. In the case of the chirp, the recorded signal must be correlated with the input signal to obtain the impulse response, hence this being an indirect method.

Knowing the response of the cylinder is possible to, one more time, calculate the frequency response and compare the results when the input signal is the knock of a hammer and the linear chirp. But first, it's necessary to alter the setup a little by adding a contact speaker to reproduce the linear chirp.

4.2   Experimental setup

The experimental setup for this experiment is practically the same as the one presented in the last chapter on section 3.2 but with the addition of a contact speaker. The setup now consists of the cylinder, that is the system from which the frequency response will be acquired, a contact speaker to reproduce the chirp wave into the surface of the cylinder replacing the knock of the hammer, a microphone to record the signal, a soundboard responsible to acquire the recorded signal and to send the linear chirp generated by the MATLAB to the contact speaker. Figures 4.1 and 4.2 show the assembled setup and the equivalent block diagram.

Figure 4.1: Experimental setup with a contact speaker to transmit the chirp signal to the cylinder.
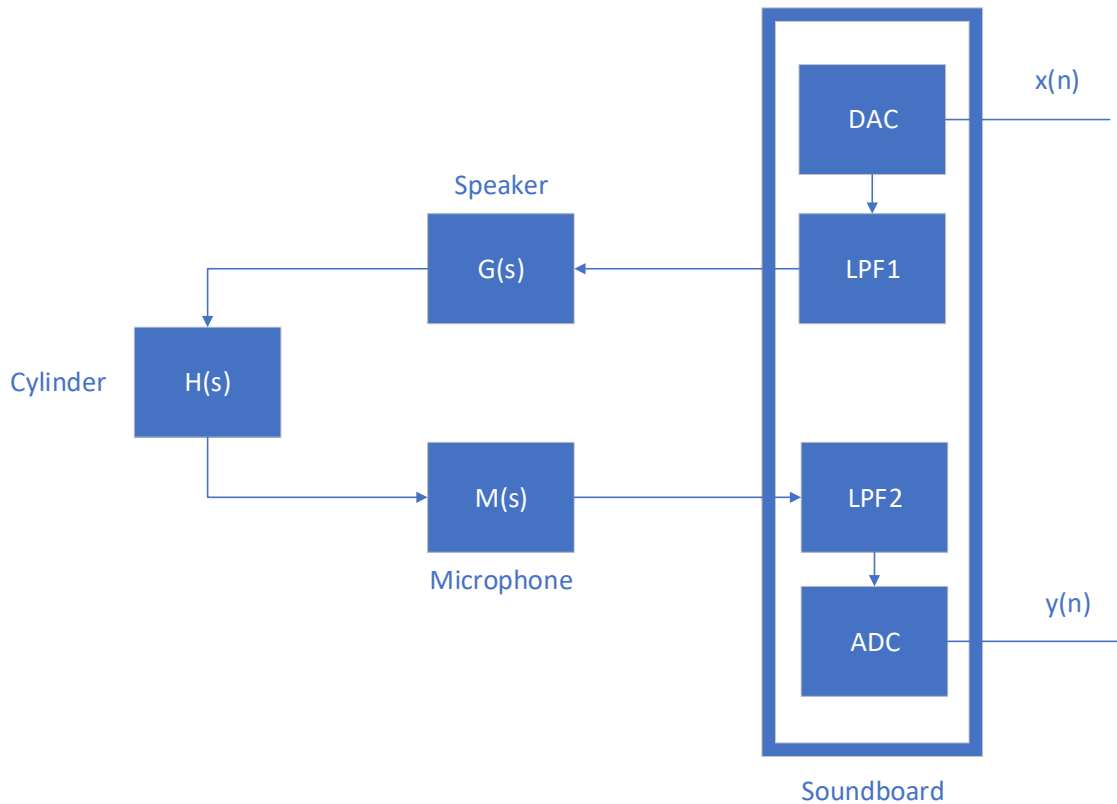
Figure 4.2: Block diagram of the experimental setup with the contact speaker.

To substitute the knock of a hammer, the input signal will now be a linear chirp with a frequency sweep ranging from $20Hz$ to $20kHz$ which allow us to understand the frequency response of the cylinder in this range, in order to confirm if the chirp is a good approximation of the impulse generated by the hammer. The signal is digital, being generated by MATLAB. The soundboard converts the signal to analog domain through the DAC and sends to the contact speaker, that is responsible to its reproduction. The microphone records the signal during 100 seconds, being this value chosen to guarantee that all frequencies have time to manifest since, by previous observations of the spectrogram of the impulse response generated by the hammer, the frequencies with higher magnitude could manifest until 10 seconds. The signal recorded by the microphone is processed by the ADC of the soundboard where it's converted to digital and sent to the PC to be processed by MATLAB, where it's possible to correlate the recorded signal with the chirp, to calculate the impulse response and the frequency response of the cylinder.

4.2.1 Hardware and Software

The experimental setup presented in this chapter is quite similar to the one presented in the last Chapter. The only software used in this work continues to be the MATLAB but in

the hardware section, there is a new addition: a contact speaker.

Figure 4.3: Vibe-Tribe Ninja 3D Speaker

The contact speaker is a Vibe-Tribe Ninja $3D$ Speaker. The reason for choosing this speaker is because of its "Vibration Resonance" technology. This technology transforms electromagnetic pulses into mechanical vibrations. These vibrations are transferred to any surface, transforming the surface into an acoustic source and spreading sound in an omnidirectional way, with an output power of $3W$ Root Mean Square (RMS)[23].

The type of surface alters the timbre of the sound reproduced by the speaker. Follows a table provided on [23] comparing the sound experience for different surfaces.

Table 4.1: Sound experience for different types of surfaces. Source:[23]

Surface	Sound experience
$Wood$	Rich Bass sound
$Metal$	Strong Bass sound
$Paperboard$	Vinyl effect
$Glass$	Clean and clear sound
$Hollowwall$	Good spacious sound

The hammer generates a mechanical vibration that is approximately an impulse while the speaker is responsible to generate a mechanical vibration that is approximately a linear chirp.

4.3 Detection with a linear chirp

4.3.1 Impulse and Frequency Response

Unlike the last chapter, where an impulse was generated with the knock of a hammer, this time, the input signal will be a linear chirp generated by a contact speaker. Since the contact speaker transforms the electromagnetic pulses in mechanical vibrations, the method to generate an impulse is the same but, instead of an impulse, we have a linear chirp.

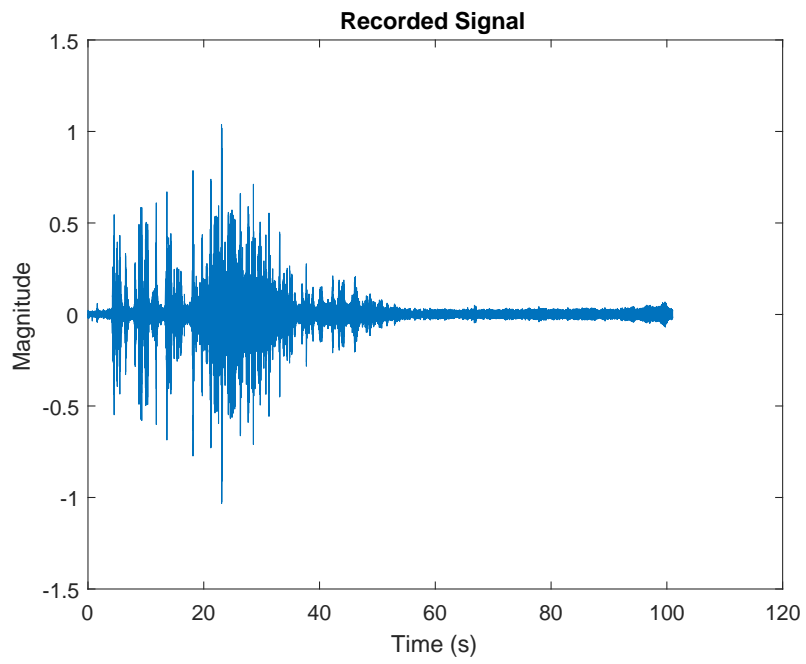The recorded signal obtained is shown by Figures 4.4, 4.5 and 4.6.

Figure 4.4: Recorded output of the full cylinder.
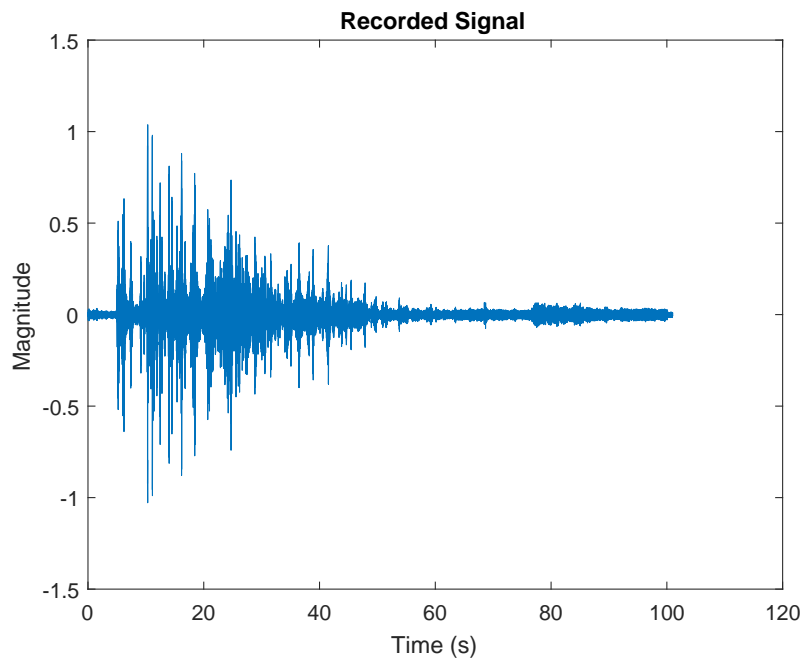
Figure 4.5: Recorded output of the half-full cylinder.
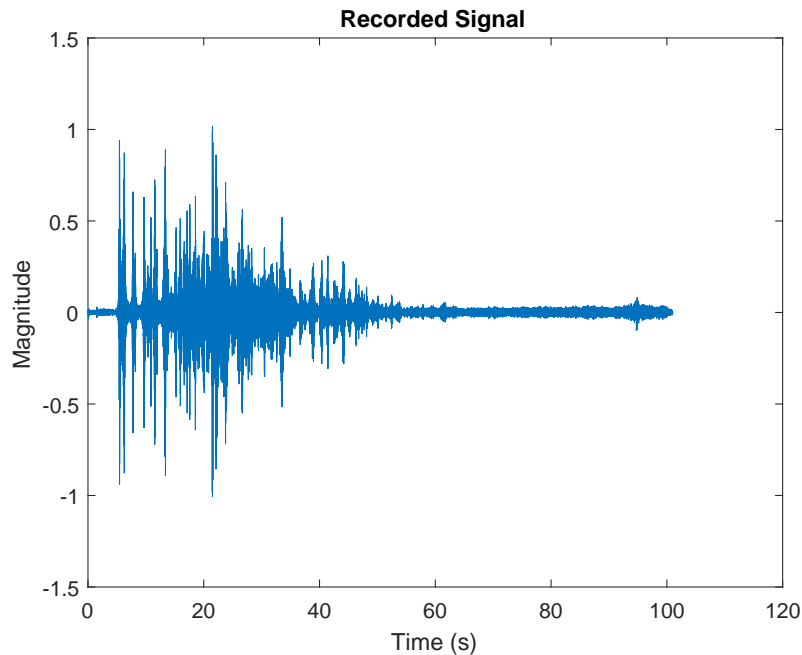
Figure 4.6: Recorded output of the empty cylinder.

Is possible to observe that, unlike the previous experiment where the recorded signal was the direct impulse response of the cylinder, in this case, the recorded signal is the response of the system when the input signal is a linear chirp. This response is different from the previous one, because of the application of a linear chirp as the input signal that, per se, isn't considered an impulse. However, the autocorrelation of a linear chirp is approximately an impulse. When the autocorrelation of a signal is approximately an impulse and that signal is the input of the system, the correlation between the input and the output is the response of the system.

The impulse response of the cylinder obtained by the correlation of the recorded signal with the linear chirp is given by Figures 4.7, 4.8 and 4.9. The autocorrelation of the linear chirp is also shown.

It's possible to observe through Figures 4.7, 4.8 and 4.9 that exists a lag (delay of samples) between the autocorrelation of the linear chirp and the cross-correlation between the recorded signal and the linear chirp. This lag is a delay caused by the soundboard and has a different value every time. To measure the real impulse response of the cylinder first is necessary to correct this delay (refer to the MATLAB code in the appendix). Figures 4.10, 4.11 and 4.12 show the impulse response without delay samples.

42
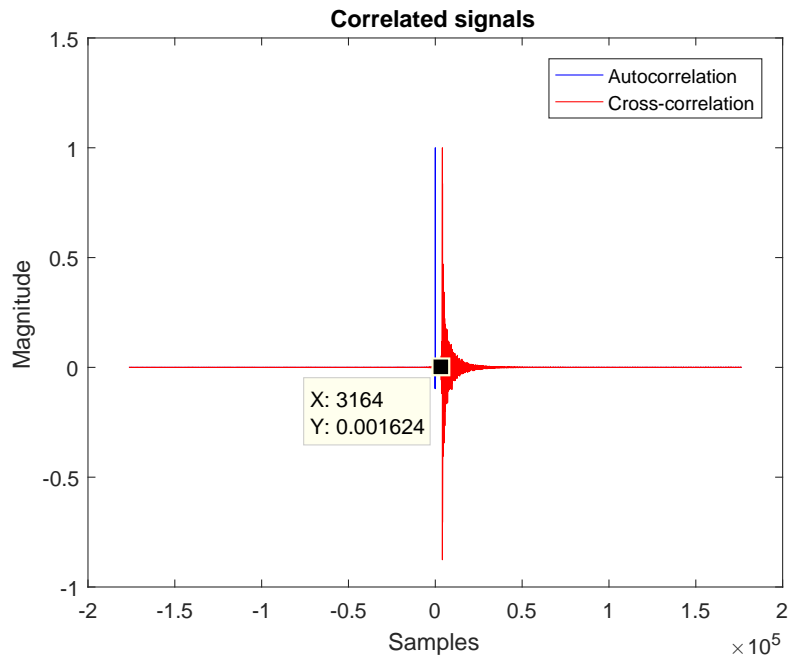
Figure 4.7: Impulse response of the full cylinder obtained by the cross-correlation of the recorded signal with a linear chirp, as well as the autocorrelation of the chirp.
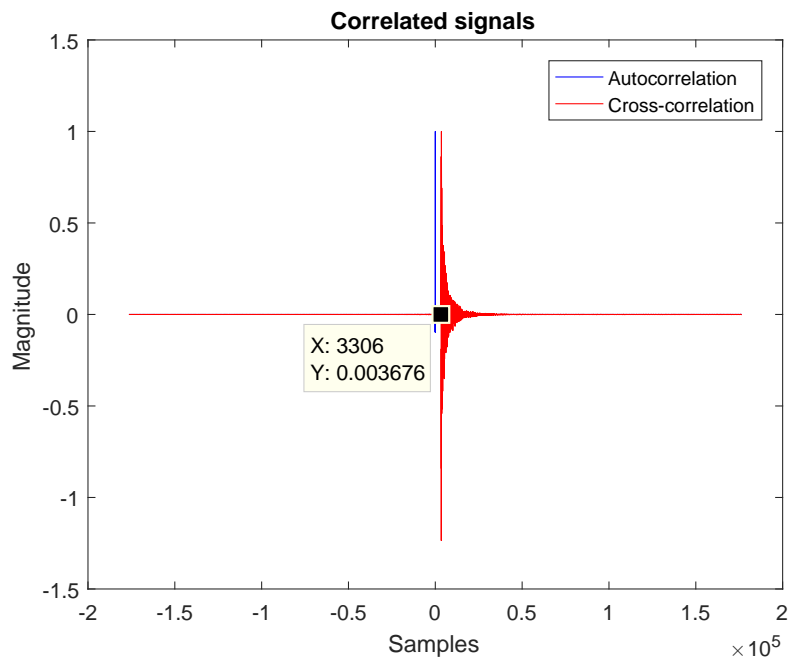
Figure 4.8: Impulse response of the half-full cylinder obtained by the cross-correlation of the recorded signal with a linear chirp, as well as the autocorrelation of the chirp.
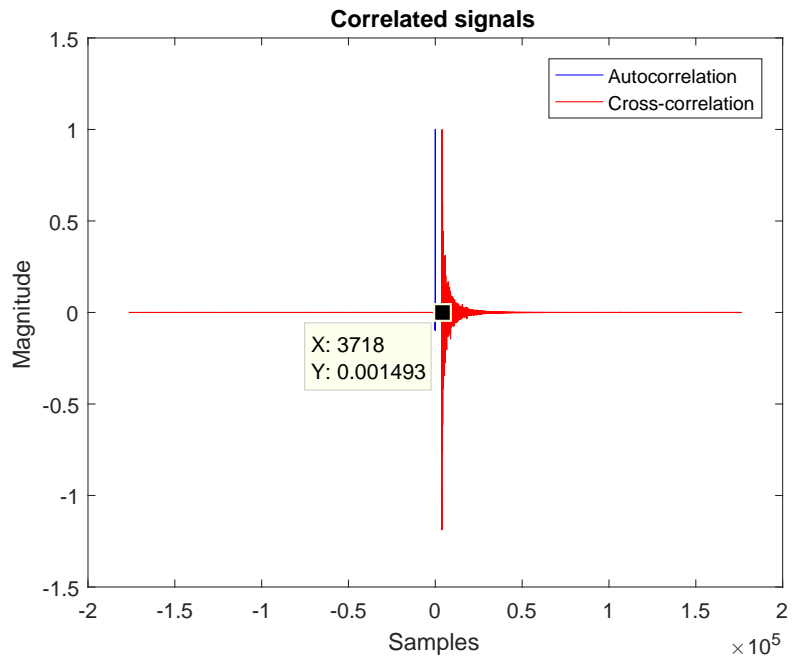
Figure 4.9: Impulse response of the empty cylinder obtained by the cross-correlation of the recorded signal with a linear chirp, as well as the autocorrelation of the chirp.
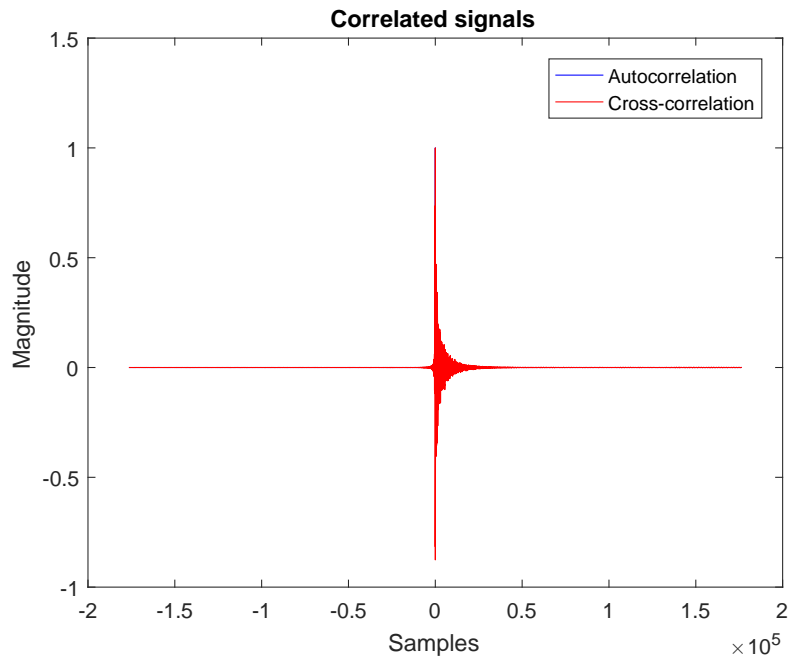
Figure 4.10: Impulse response of the full cylinder without the delay.
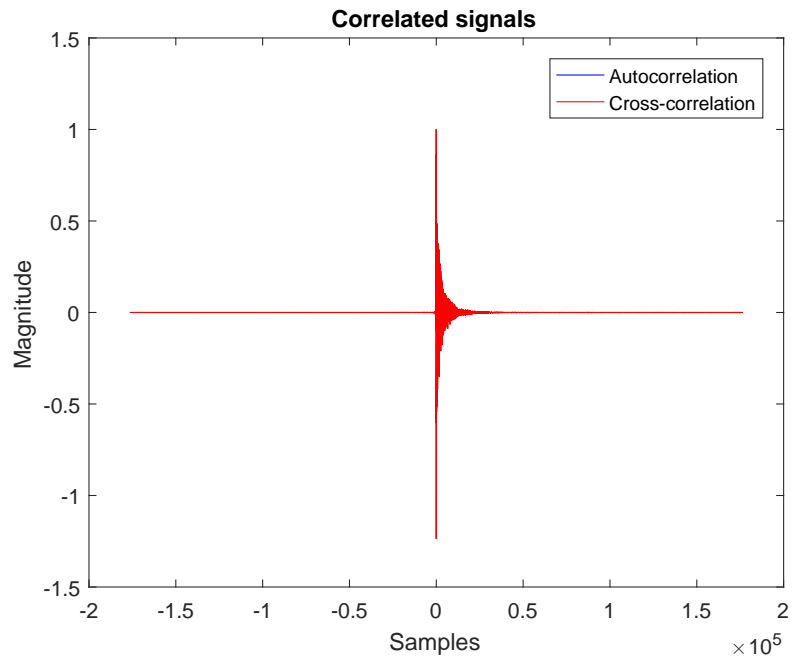
Figure 4.11: Impulse response of the half-full cylinder without the delay.
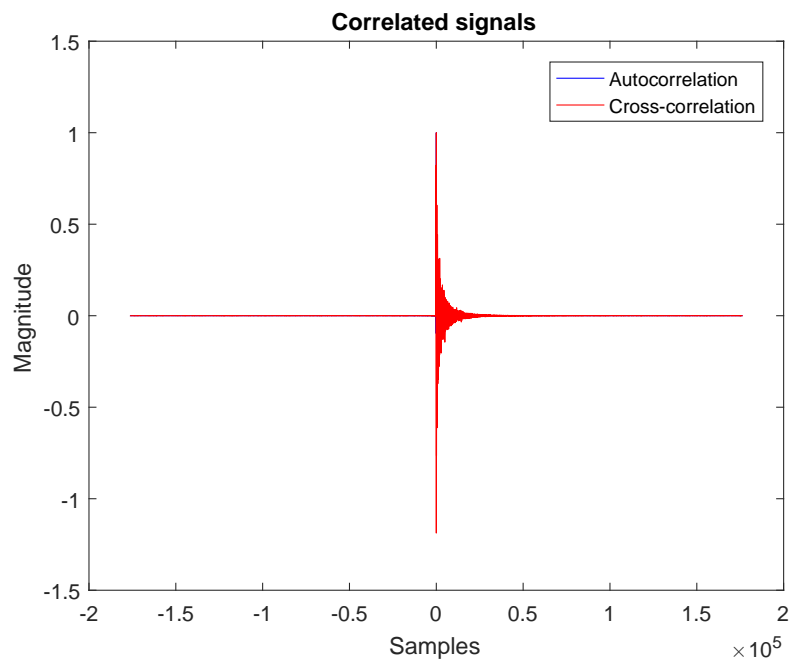
Figure 4.12: Impulse response of the empty cylinder without the delay.

After the correction of the delay, is possible to measure the frequency response of the cylinder, being the results presented by Figures 4.13, 4.14 and 4.15.
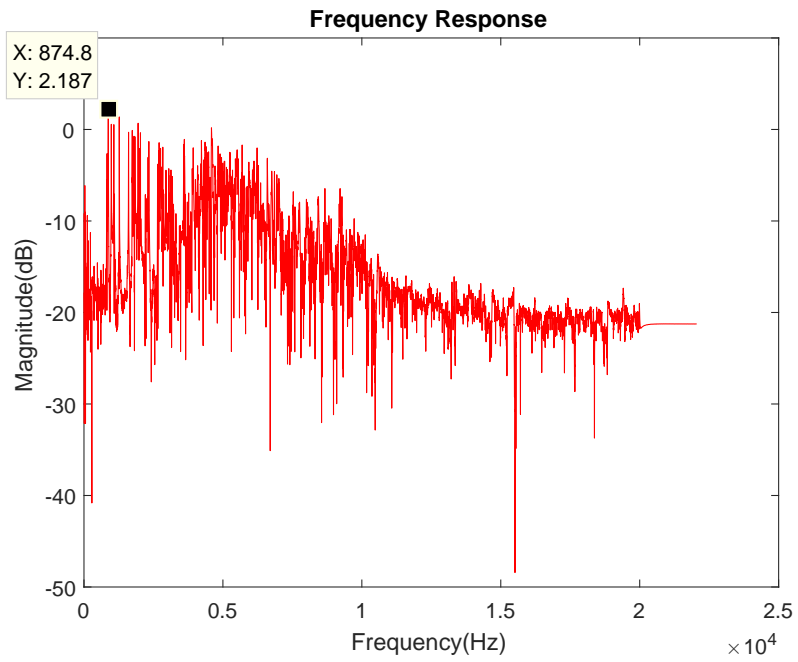
Figure 4.13: Frequency response of the full cylinder without the delay.
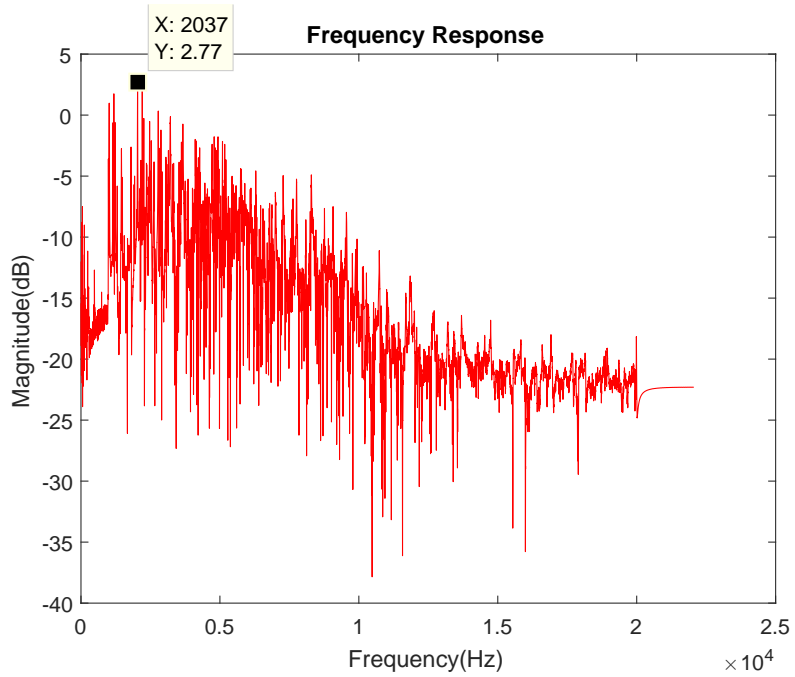
Figure 4.14: Frequency response of the half-full cylinder without the delay.
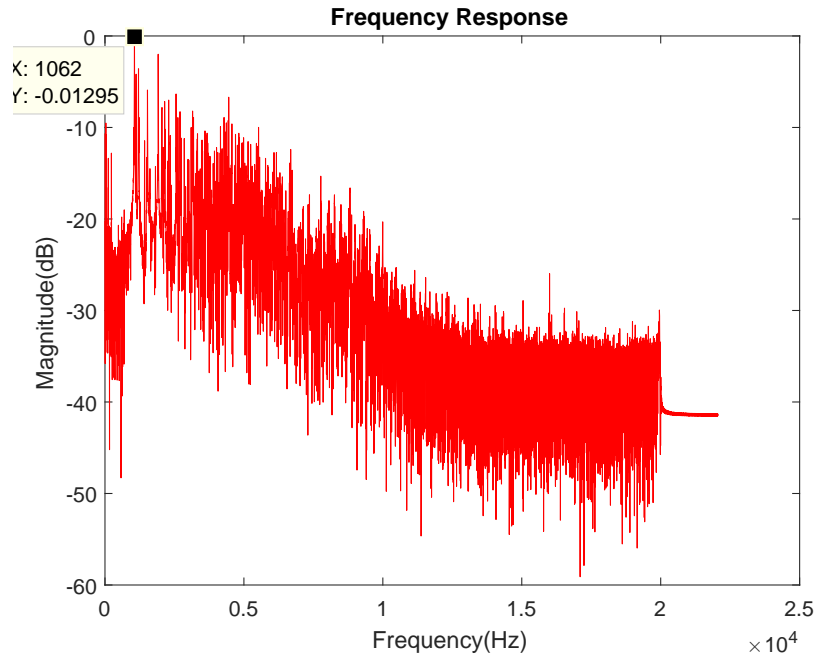
Figure 4.15: Frequency response of the empty cylinder without the delay.

When the vibration is generated by a linear chirp, is possible to observe, through the plot of the frequency response of the cylinders, that there are more frequencies with a higher magnitude in comparison with the direct method that is the knock of a hammer. These frequencies are the resonant frequencies of the cylinder. Since the chirp is a linear frequency sweep, more frequencies are excited when compared with the knock of a hammer. This fact doesn't cause any problem for the detection system if the frequencies with a higher magnitude are the same or similar to the ones obtained previously in the last chapter.

With the use of a linear chirp, the frequencies with a higher magnitude for the full, half-full and empty cylinders are, respectively, $874.8Hz$, $2037Hz$, and $1062Hz$. Although the frequency response of the full and the empty cylinders are similar to the one obtained with the knock of a hammer ($863.3Hz$ for the full cylinder and $1058Hz$ for the empty cylinder), the frequency with the higher magnitude for the half-full cylinder is $2037Hz$.

Previously in the last chapter, on Figures 3.13, 3.14 and 3.15, it was possible to observe that the frequency with a higher magnitude had a longer duration than the others, which means that the frequency with a higher magnitude will always have a time span that is superior to the others frequencies that manifest on the cylinder. When the vibration happens, several frequencies with high spectral energy manifest, fading away almost instantly, remaining only the frequencies that have a high PSD through a high duration of time. That is to say, by analyzing the "tail" of the impulse response and ignoring the first samples, is possible to measure the real frequency response of the system.

With the direct impulse response, even without discard of samples, there is a frequency with a higher magnitude that stands out, in comparison with all the others. In this case, such is not possible to observe, being necessary the analysis of the spectrogram of the signal and its corresponding tail. Follows the impulse response of the cylinder and its respective "tail".

47
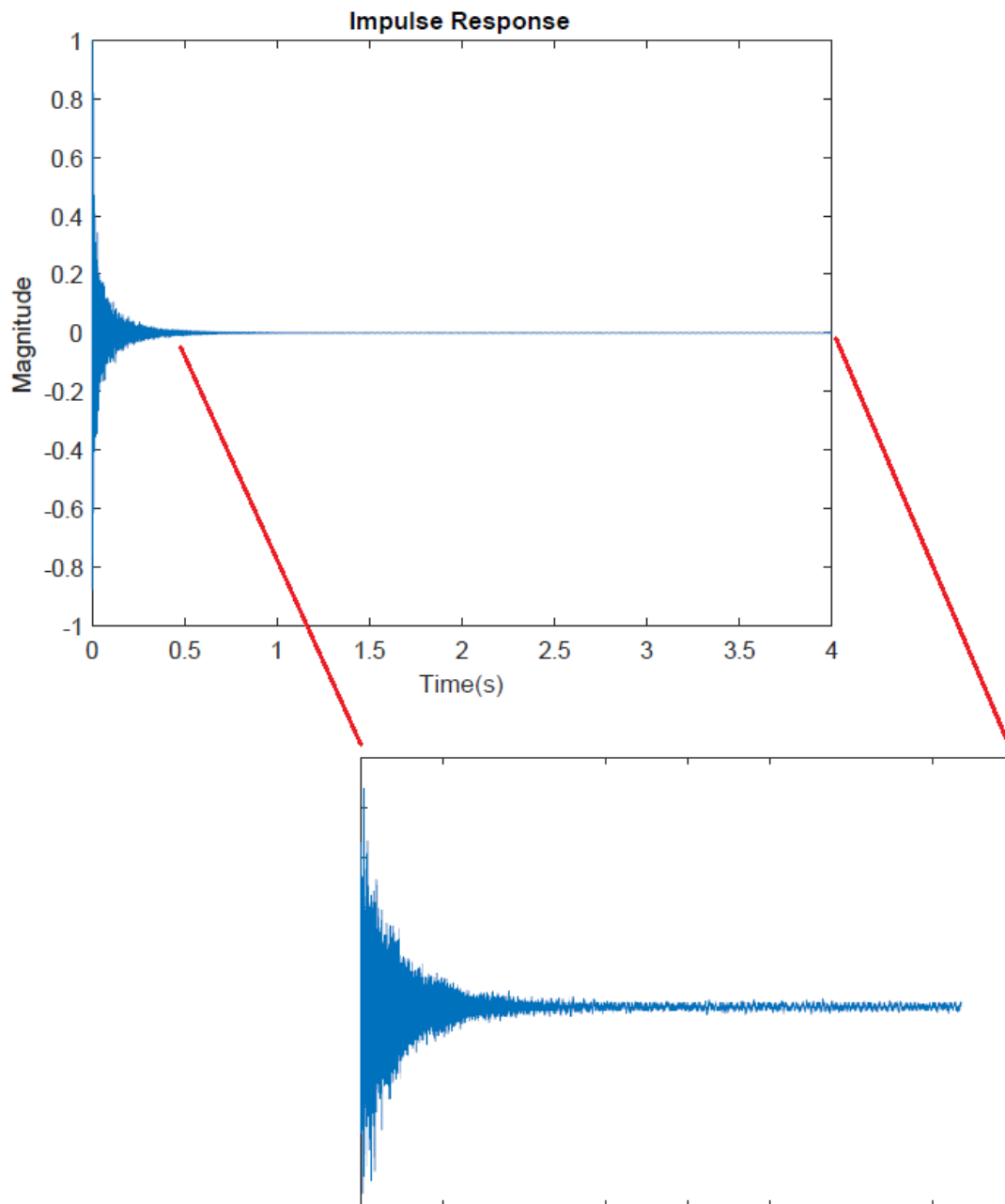
Figure 4.16: Impulse response of the full cylinder and its "tail".
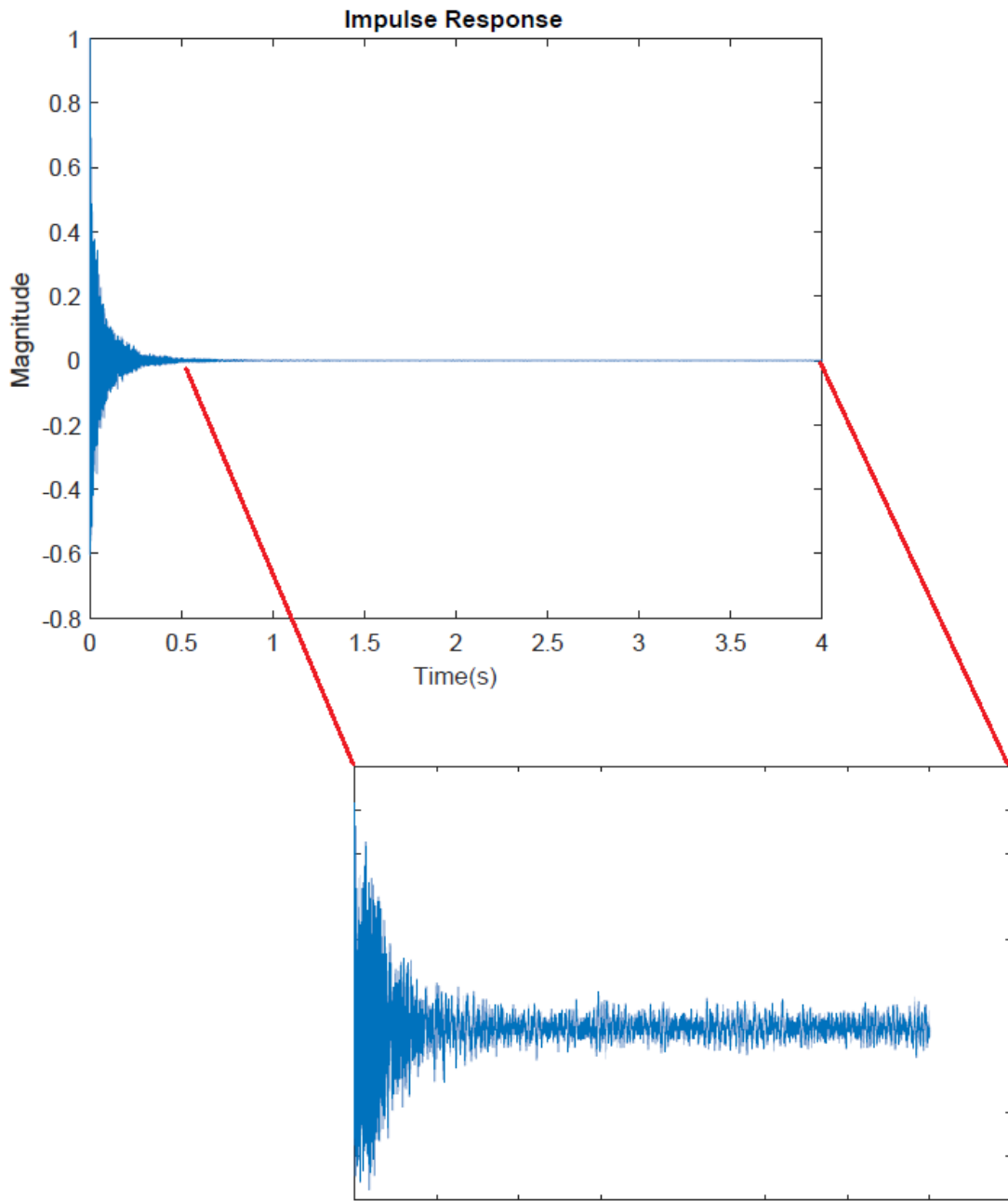
Figure 4.17: Impulse response of the half-full cylinder and its "tail".
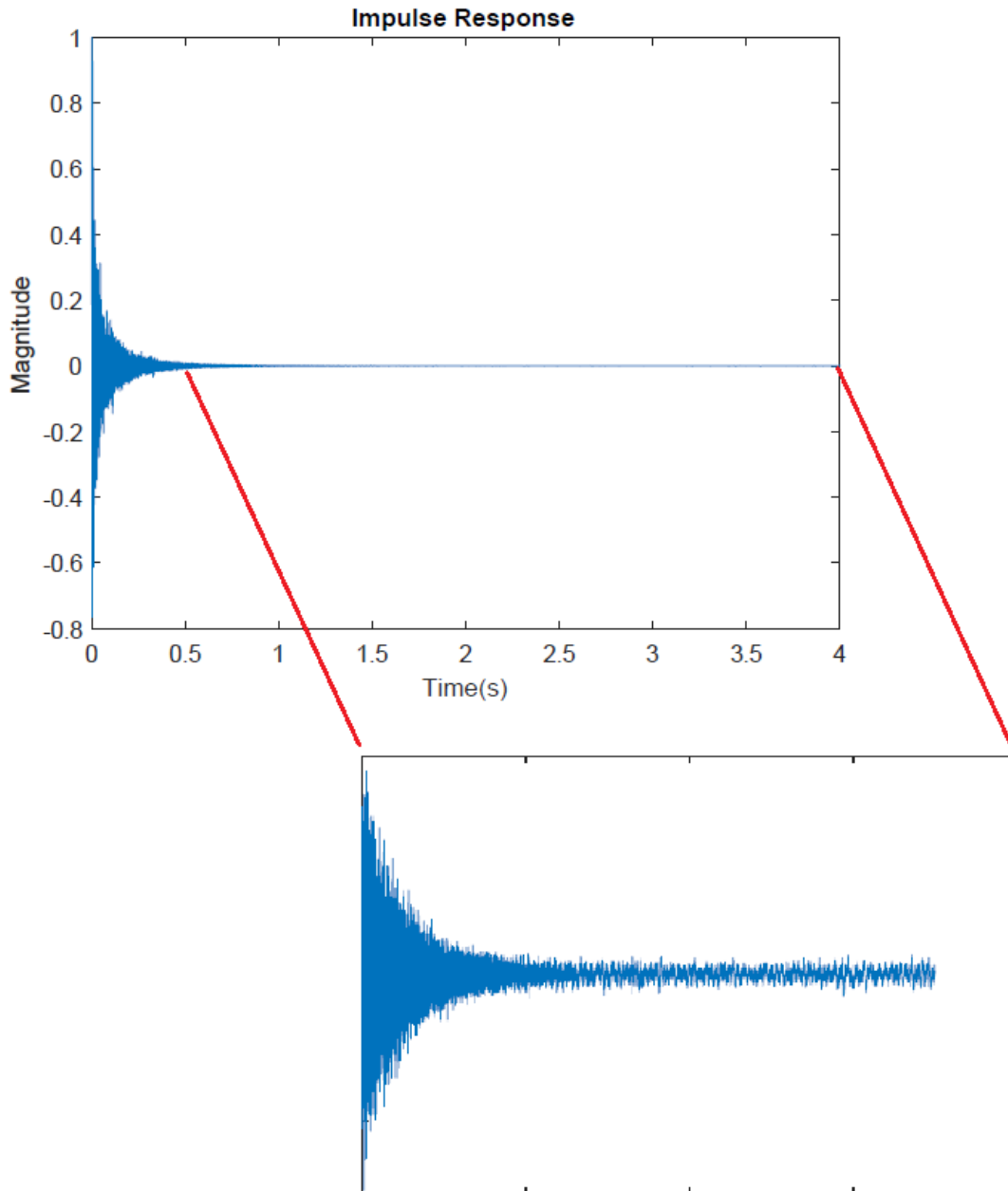
Figure 4.18: Impulse response of the empty cylinder and its "tail".

To measure the correct frequency response of the system, the first half of a second was discarded, since the error on those initial seconds is high, mainly because of the several frequencies that manifest initially. At the same time, if more samples would have been discarded, it would compromise the resolution of the measured data, because the processed signal would have more noise than information.

The spectrogram of the impulse response of each cylinder and the spectrogram of the "tail" of the impulse response can be observed in the following figures.
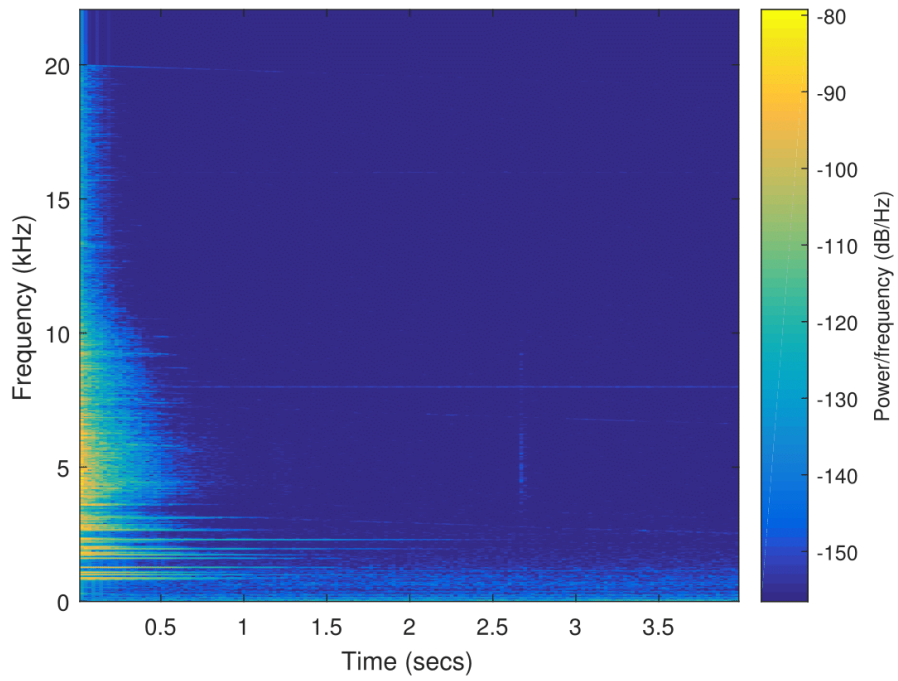
Figure 4.19: Spectrogram of the entire impulse response of the full cylinder.
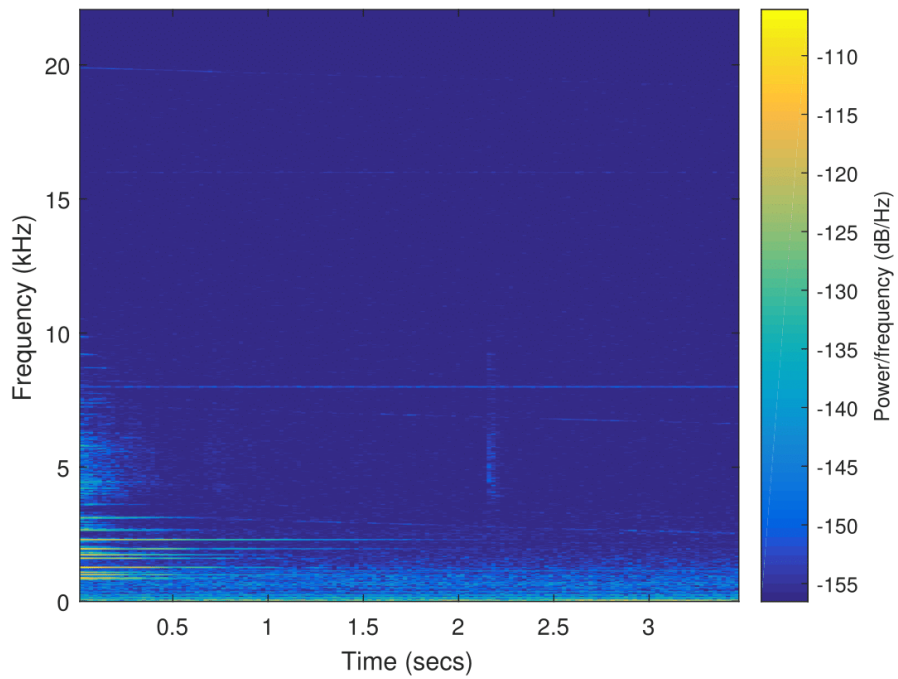
Figure 4.20: Spectrogram of the impulse response with the first 0.5 seconds discarded of the full cylinder.
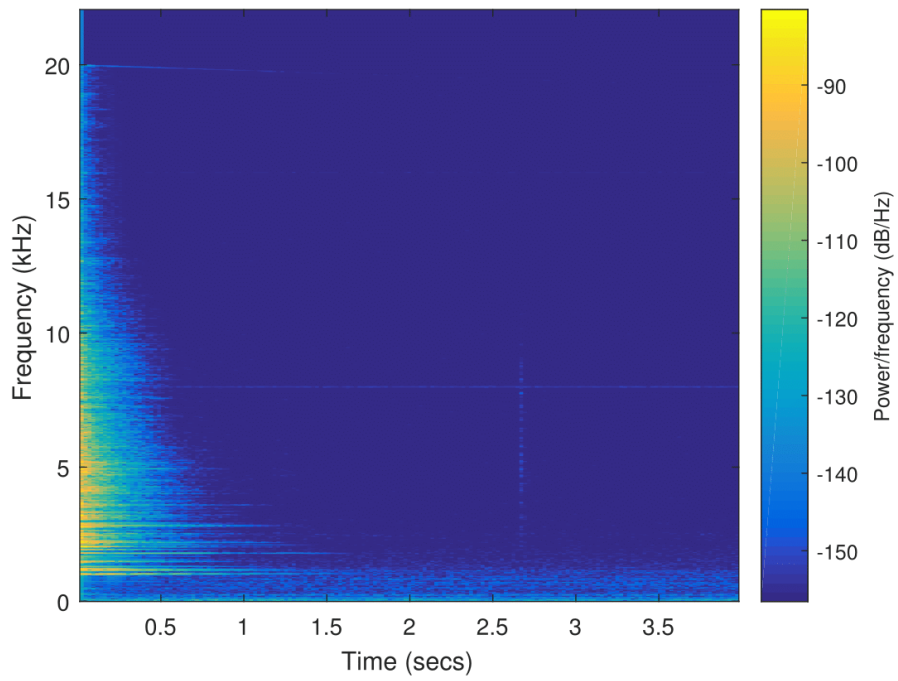
Figure 4.21: Spectrogram of the entire impulse response of the half-full cylinder.
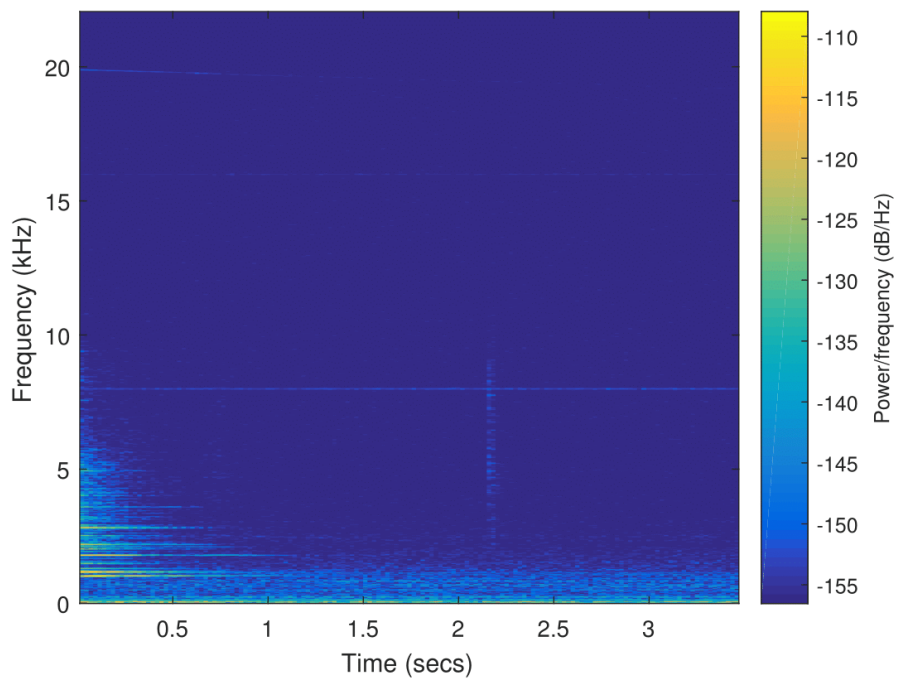
Figure 4.22: Spectrogram of the impulse response with the first 0.5 seconds discarded of the half-full cylinder.
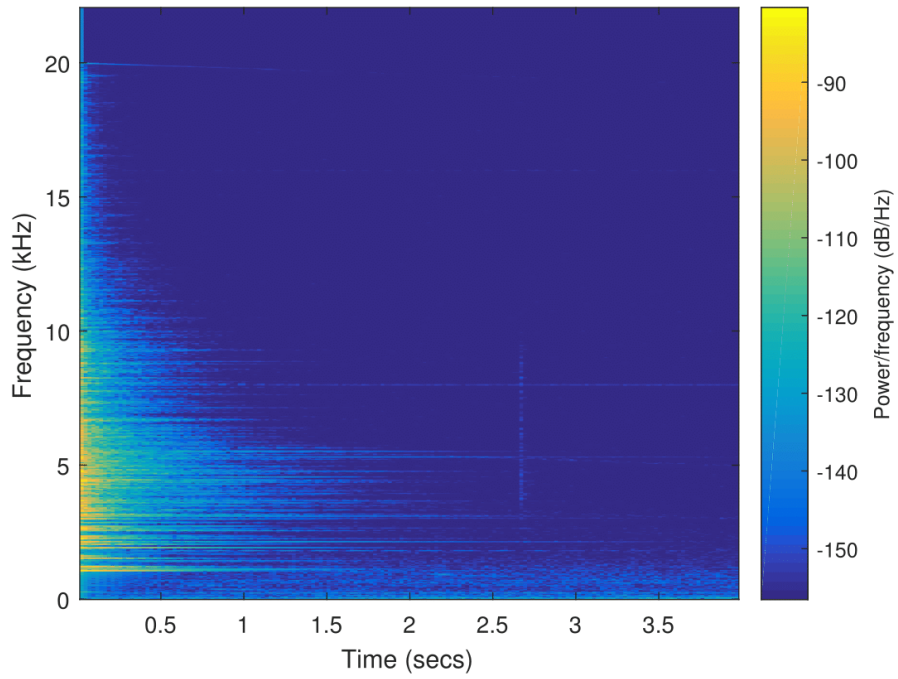
Figure 4.23: Spectrogram of the entire impulse response of the empty cylinder.
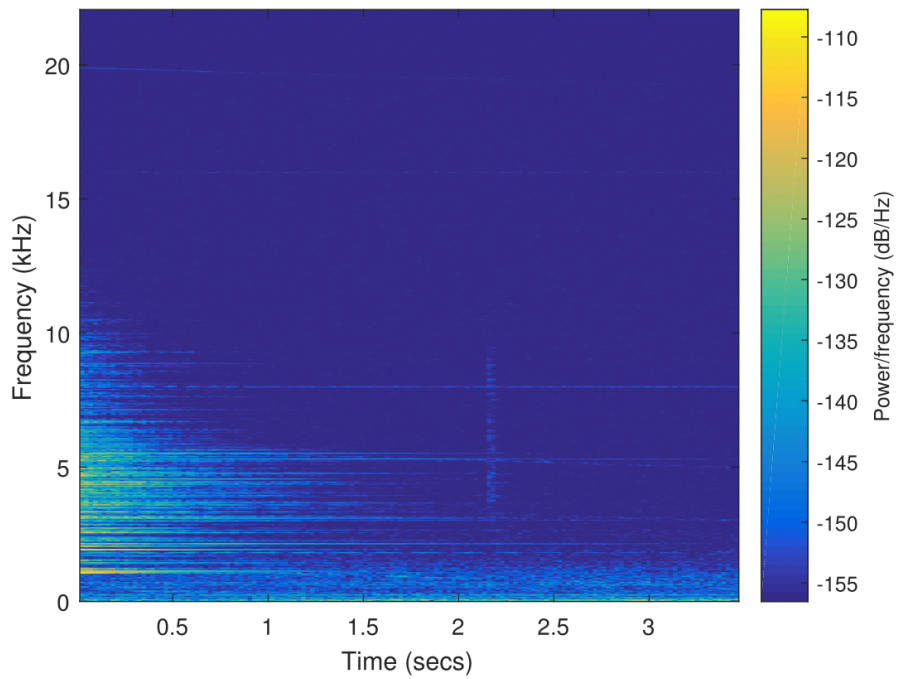
Figure 4.24: Spectrogram of the impulse response with the first 0.5 seconds discarded of the empty cylinder.

The frequency response of the "tail" of the impulse response, when the first 0.5 seconds are discarded, is given by figures 4.25, 4.26 and 4.27.
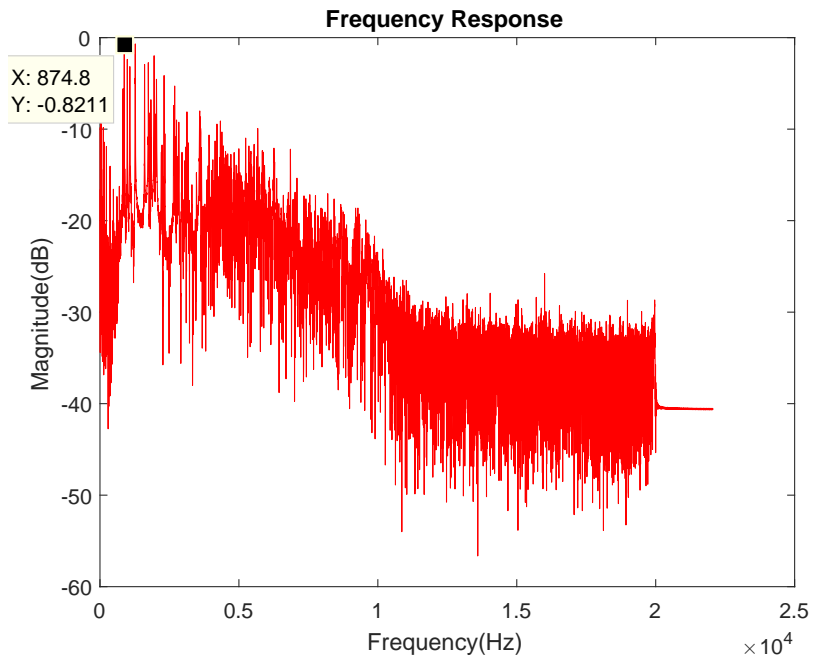
Figure 4.25: Frequency response of the "tail" of full cylinder.
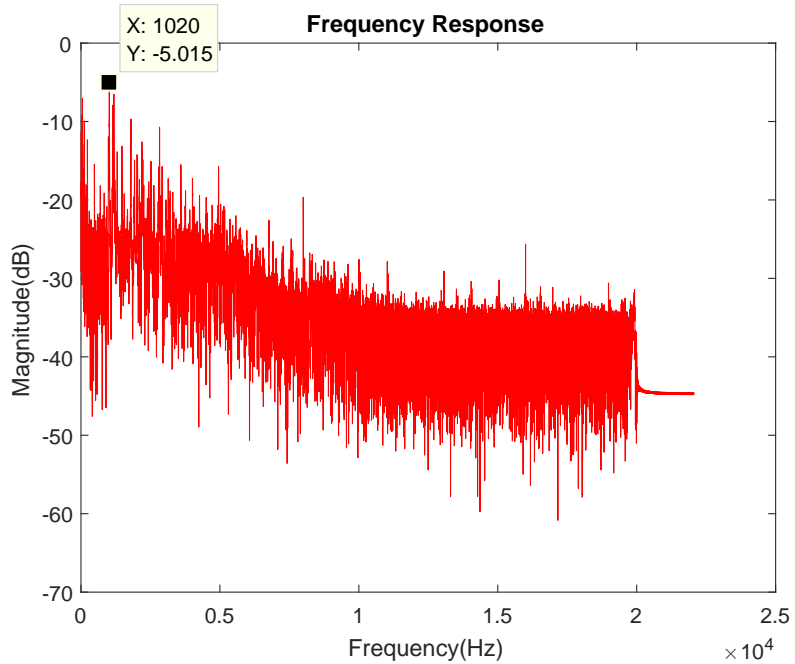
Figure 4.26: Frequency response of the "tail" of the half-full cylinder.
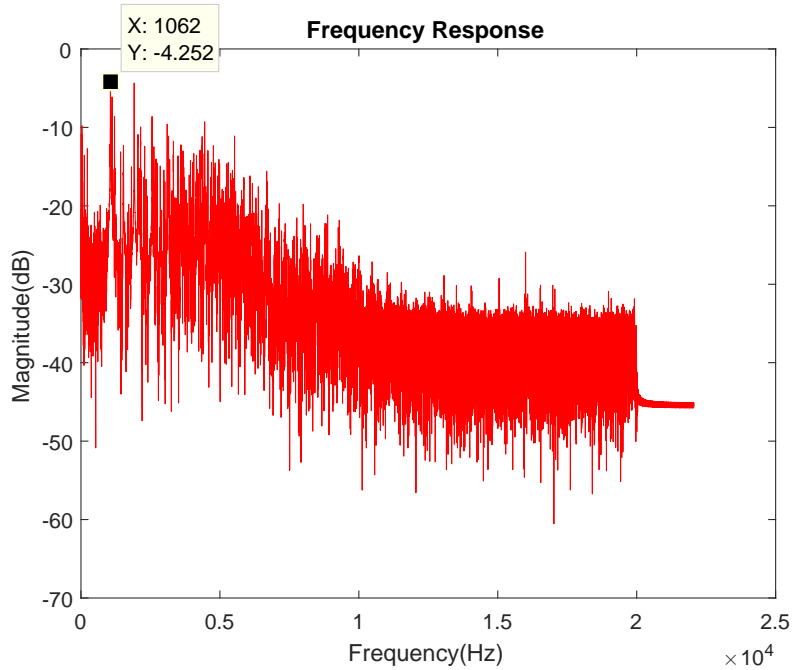
Figure 4.27: Frequency response of the "tail" of the empty cylinder.

Table 4.2: Weight and its corresponding frequency of the full impulse response and the impulse response with the initial 0.5 seconds discarded.

Weight	Frequency (no discard of samples)	Frequency (discard of samples)
$Full$	$874.8Hz$	$874.8Hz$
$Half - full$	$2037Hz$	$1020Hz$
$Empty$	$1062Hz$	$1062Hz$

Through the analysis of the frequency response of the "tail" of the impulse response, the value of the frequency with a higher magnitude is $874.8Hz$, $1020Hz$ and $1062Hz$ for the full, half-full and empty cylinders respectively.

It is possible to observe that the frequency with the higher magnitude of the half-full cylinder changed, proving that the frequency of $1020Hz$ had a higher PSD when compared with the frequency of $2037Hz$. The frequencies of the full and the empty cylinder with the higher magnitude are still the same, which gives veracity to the frequency response of the half-full cylinder.

Chapter 5

Conclusions and future work

5.1   Conclusions

In conclusion, until now, a non-intrusive method to measure the liquid level of a gas cylinder would rely on the use of a hammer, that would generate the impulse response of the system. To replace the hammer and still acquire a similar impulse response, a linear chirp with a frequency range of $20Hz$ to $20kHz$ was chosen, being the results similar to the two methods.

Before the start of the tests, it was necessary to confirm the linearity and time invariance of the system. A setup was developed where the input of the system was a sinusoidal wave with a distinct frequency, being the output a frequency component with the same distinct frequency as the input. The same can be seen when the input is a sum of sinusoids with distinct frequencies, being the output given by the frequency components of each sinusoid.

Since the cylinders were LTI, it was possible to measure the impulse response of each cylinder through the knock of a hammer and map the weight of each cylinder, with its corresponding frequency, giving us a way to establish a measurement model of a cylinder through its frequency response.

By substituting the hammer for a linear chirp, the hassle of the knocking disappears, giving us a more practical way of measurement. The impulse was now generated by a contact speaker that transform the electromagnetic waves in vibration, causing the necessary stimulus that allows the measurement of the impulse response of the cylinder and subsequently its frequency response.

Since the soundboard has a considerable lag of samples that change with each run of the script, first was necessary to correct that lag to measure the real impulse response of the system, being the initial moments of that impulse response later discarded because the dominant frequencies are on the tail of the impulse response.

With each frequency response measured, It's possible to observe through Table 5.1, that the linear chirp has a frequency response where the frequency with the higher magnitude is similar to frequency response when the input signal is a hammer.

Table 5.1: Comparison of the weight vs frequency for the two measurement methods

Weight	Frequency (direct method)	Frequency (indirect method)
$Full$	$863.3 Hz$	$874.8 Hz$
$Half - full$	$1013 Hz$	$1020 Hz$
$Empty$	$1058 Hz$	$1062 Hz$

For the full cylinder, the frequency with the higher magnitude generated by the linear chirp is $874.8.Hz$, which can be considered a good approximation of $863.3 Hz$, frequency obtained by the knock of a hammer. The same can be said about the other two cylinders. For the half-full cylinder, the frequency for the linear chirp is $1020 Hz$ being a good approximation of the $1013 Hz$ obtained with the knock of a hammer, while for the empty cylinder, the frequency with a higher magnitude for the linear chirp and for the hammer are respectively $1062 Hz$ and $1058 Hz$.

Since the frequencies are similar for the two methods, is possible to say that the linear chirp is a good approximation for the impulse response generated by the knock of a hammer.

5.2   Future Work

The initial concept of this master thesis was the development of a sensor capable to measure the liquid level of a gas cylinder. Because of some theoretical concepts that took longer to assimilate and some problems on the measurement, that persisted during the realization of this work, there wasn't time to develop the sensor. For future work, is recommended the creation of a sensor to measure the liquid level of a gas cylinder using for example a piezo sensor transducer and a low cost microprocessor. This sensor would be connected through a database using the concept of the Internet of Things. A recommended setup is shown in Figure 5.1.

The Arduino would substitute the PC and the MATLAB in the generation and the transmission of a linear chirp. The piezoelectric speaker and the electret microphone are a cheap substitute for the Behringer $ECM8000$ and the Vibe-Tribe Ninja 3D Speaker.

With a downgrade in the used material, the precision of the impulse response could suffer in comparison with a microphone and a contact speaker and so, further tests must be performed.
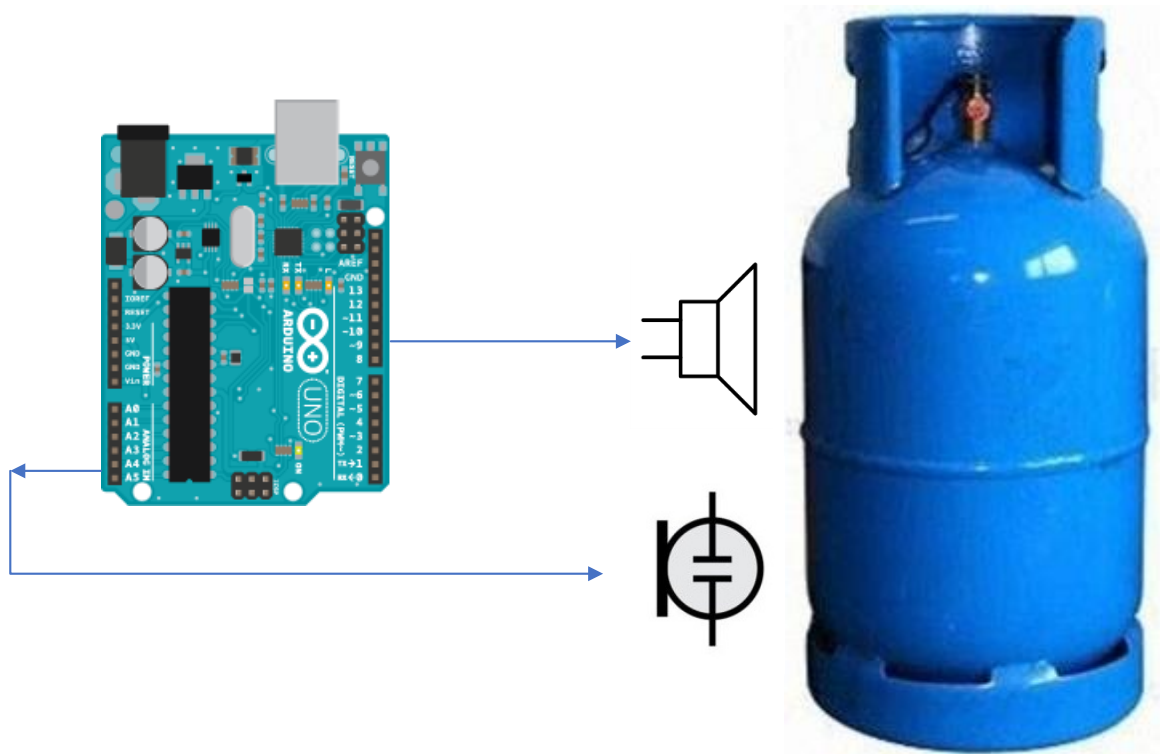
Figure 5.1: Proposed model for a sensor to measure the liquid level of gas cylinder

Appendix A

Euler-Bernoulli beam theory

A.1   Simple Beam Theory

A.1.1   What is a Beam?

A beam is an element designed to support transverse loads. Transverse loads are loads that act perpendicular to the longitudinal axis of the beam and are responsible for its bending[11].
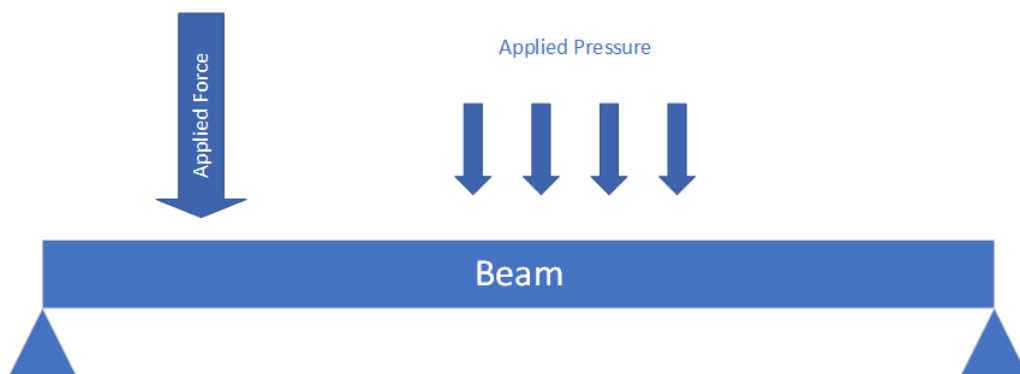
Figure A.1: A generic beam with applied pressure and applied force.

To prevent twisting and to guarantee that the beam will only bend, It's necessary to assume a longitudinal plane of symmetry for the beam, like the one shown in Figure A.2.
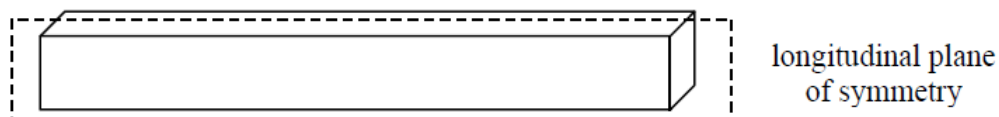
Figure A.2: Beam longitudinal plane of symmetry. Source:[11]

When there is a transverse load applied on the beam and it's applied downwards, the beam bends. This bending is responsible for a contract in length on the top of the beam and an extension, also in length, on the bottom part. Even though a bending happens, in the

61

beam, continues to exists a plane where the beam doesn't change, called the neutral surface. When the neutral surface intersects with the longitudinal plane of symmetry is called the axis of the beam.
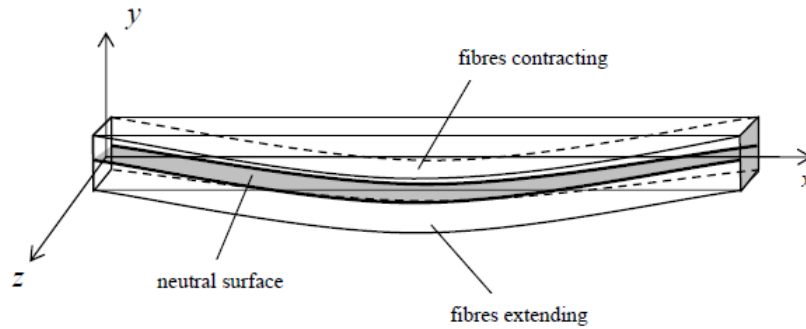
Figure A.3: Beam neutral axis. Source:[11]

It's necessary to add a coordinate system to the beam to an easy understanding of the direction of the forces applied to it.

A.1.2 Moments and Forces in a Beam

When Inspecting any cross-section of a beam it's possible to observe the effects of normal and shear stresses that act on each side of the section, being these stresses in equilibrium. The value of the normal stress σ changes over a section while that section is bending. That happens because in one part of the section the stress will be tensile, while on the other part will be compressive, resulting in a bending moment called M. The shear stress τ that also acts over this section, also results in a shear force designated by V[11].

Figure A.4 shows how these forces act in the cross-section.
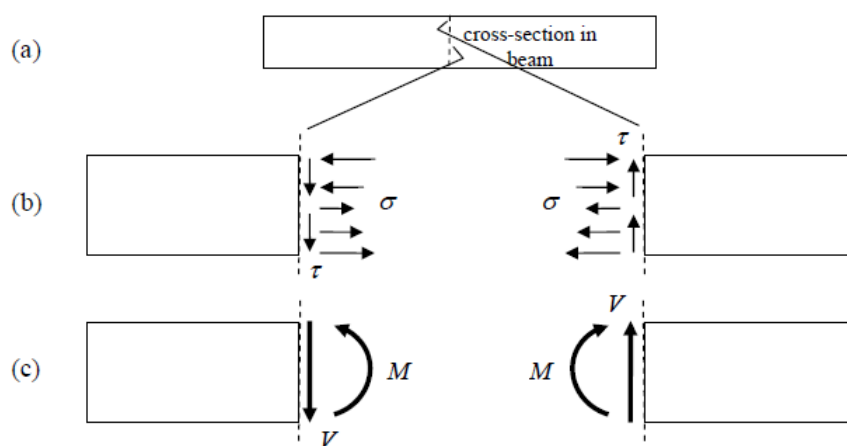
Figure A.4: Stresses and moments that act over a cross-section of a beam; (a) - Traditional cross-section, (b) - Normal and Shear Stresses acting over the cross-section, (c) - The resultant Moment and Shear Force resultant from the normal stress and the shear stress. Source:[11]

A.1.3   The Relationship between the forces applied on the beam

When we consider a small section of the beam with a width of Δx, if a distributed load $p(x)$ is applied to the section, is possible to describe the forces that act on the beam (being these forces the shear force and the bending moment) and how they interact with the load[11]. The following figure shows this relationship.
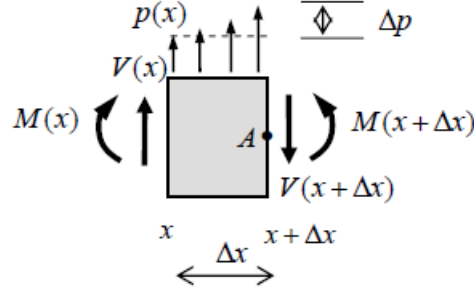
Figure A.5: Forces that act on a small section of the beam. Source:[11]

As shown in Figure A.5, on the left side of the section, the distributed load assumes the value of $p(x)$, the shear force is $V(x)$, while $M(x)$ corresponds to the bending moment. This assumption is only valid for position x. At position $x + \Delta x$, these forces changes slightly, now depending on Δx.

Seeing that the considered section is really small, is possible to approximate the load by a linear variation over the section, considering now a variation between 0 at position x and Δp at position $x + \Delta x$. With this simplification, the equation of equilibrium of the vertical forces becomes:

$$V(x) + p(x)\Delta x + \frac{1}{2}\Delta p \Delta x - V(x + \Delta x) = 0 \tag{A.1}$$

which is the same as:

$$\frac{V(x + \Delta x) - V(x)}{\Delta x} = p(x) + \frac{1}{2}\Delta p \tag{A.2}$$

When the left side of the small section tends to zero, the left side of the equation A.2 becomes the definition of the derivative. On the other hand, Δp also tends to zero, transforming equation A.2 on:

$$\frac{dV}{dx} = p(x) \tag{A.3}$$

Where we have the relation between the shear forces and the distributed load.

Now, considering moment equilibrium, we have:

$$\frac{M(x + \Delta x) - M(x)}{\Delta x} = V(x) + p(x)\frac{\Delta x}{2} + \Delta p\frac{\Delta x}{6} \tag{A.4}$$

As previously observed, when the left side of the section tends to zero, the left side of the equation also becomes a derivative, while in the right side Δx and Δp tends to zero, which becomes:

$$\frac{dM}{dx} = V(x) \tag{A.5}$$

We now have the relationship between the shear force and the bending moment.

A.1.4 Deformations in beams

The bending moment at a cross-section happens when there's a distribution of normal stress. To understand how this distribution occurs is necessary to locate the position of the neutral axis. For this, the deformation is a parameter to take into consideration. Thus, it is necessary to assume two more properties[11].

- The plane in a deformed beam remains perpendicular when there is a deflection.

- Deformation happens only on the x-axis (longitudinal strain ϵ_{xx}) while on the y-axis (transverse strain ϵ_{yy}) is neglected.

The longitudinal strain is then:

$$\begin{aligned}
\epsilon_{xx} &= \frac{\Delta x' - \Delta x}{\Delta x} \\
&= \frac{(R - y)\Delta\theta - R\Delta\theta}{R\Delta\theta} \\
&= -\frac{y}{R}
\end{aligned} \tag{A.6}$$

Where y is the distance from the neutral axis and R is the radius of curvature from the deflection curve. When R is large, the curvature is small as well as the strain. When R is small, the curvature is large, leading to a large strain.
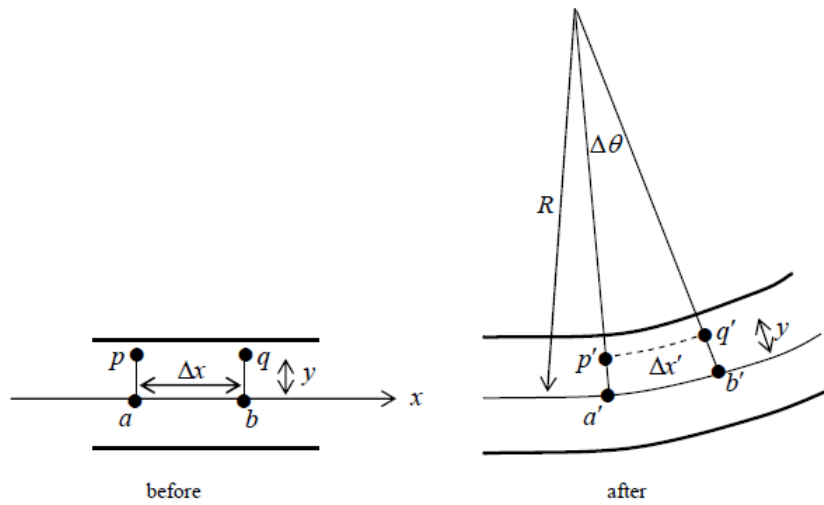
Figure A.6: Deformation in a beam. Source:[11]

Now, assuming that the beam is isotropic and elastic, the transverse normal stress σ_{yy} is neglected when compared to the flexural stress σ_{xx}. This gives us:

$$\epsilon_{xx} = \frac{\theta_{xx}}{E} \tag{A.7}$$

Which is the same as equation A.8, where E is the Young module.

$$\theta = -\frac{E}{R}y \tag{A.8}$$

Finally, when the resultant force of the normal stress distribution and the resultant moment M are considered, with some simplifications, the flexural stress in a beam is given by the expression:

$$\theta = -\frac{My}{I} \tag{A.9}$$

Where I is the moment of inertia.

A.1.5 Beam Deflection

In any beam, when a deflection happens, the neutral axis change[11]. This change is represented by v, as showed in Figure A.7.
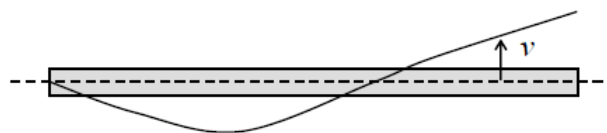
Figure A.7: Deflection of a beam. Source:[11]

The slope at any point is equal to the first derivative, while the radius of the curvature is related to the second. This relation is the curvature of the beam and is given by:

$$\frac{1}{R} = \frac{d^2v}{dx^2} \tag{A.10}$$

The curvature of the beam makes it possible to relate equation A.8 and equation A.9 which gives us:

$$M(x) = EI\frac{d^2v}{dx^2} \tag{A.11}$$

That is the moment-curvature equation.

A.1.6 Euler-Bernoulli beam equation

The Euler-Bernoulli equation describes the relationship between the applied load and the deflection of the beam[12]. It's possible to show this relation through equation A.12, by relating equations A.3, A.5 and A.11.

$$p(x) = \frac{d^2}{dx^2}\left(\frac{dv^2}{dx^2}EI\right) \tag{A.12}$$

As seen previously, p(x) is the distributed load applied to a section, E is the $Young's$ modulus and I is the moment of inertia of the beam cross-section in the direction of the y-axis. This equation allows us also to calculate the bending moment (equation A.13) and the shear force (equation A.14).

$$M(x) = EI\frac{dv^2}{dx^2} \tag{A.13}$$

$$V(x) = \frac{d}{dx}\left(\frac{dv^2}{dx^2}EI\right) \tag{A.14}$$

A.1.7 Boundary Conditions

Until now, wasn't considered any type of connection on the beam that would limit its movement, but in practice, these supports might exist to prevent the beam to crack. When a support exists, it creates a boundary condition. The most common boundaries are[12]:

- Free end.

$$Bending \quad moment = 0 \qquad Shear \quad force = 0 \tag{A.15}$$

- Simply supported end (or pinned end).

$$Bending \quad moment = 0 \qquad Deflection = v = 0 \tag{A.16}$$

- Fixed end (or clamped end).

$$Deflection = 0 \qquad Slope = \frac{dv}{dx} = 0 \tag{A.17}$$

• End connected to a linear spring, damper and mass.

$$\frac{d}{dx}\left(EI\frac{d^2v}{dx^2}\right) = a\left[kv + c\frac{dv}{dt} + m\frac{d^2v}{dt^2}\right] \qquad Bending \quad moment = 0 \qquad \text{(A.18)}$$

Where:

– for the left end of the beam $a = -1$ and for the right end $a = +1$.
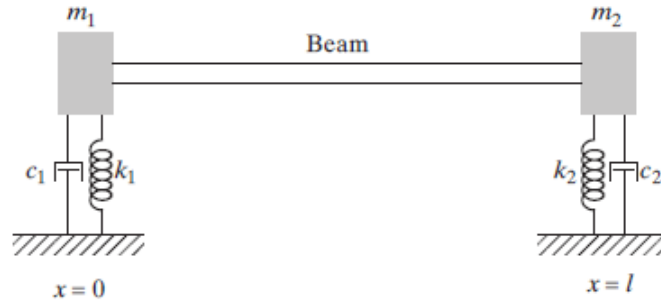
Figure A.8: Beam connected with linear springs at its ends. Source:[12]

• End connected to a torsional spring, damper and rotational inertia.

$$EI\frac{d^2v}{dx^2} = a\left[k_t\frac{dv}{dx} + c_t\frac{d^2v}{dxdt} + I_0\frac{d^3v}{dxdt^2}\right] \qquad Shear \quad force = 0 \qquad \text{(A.19)}$$
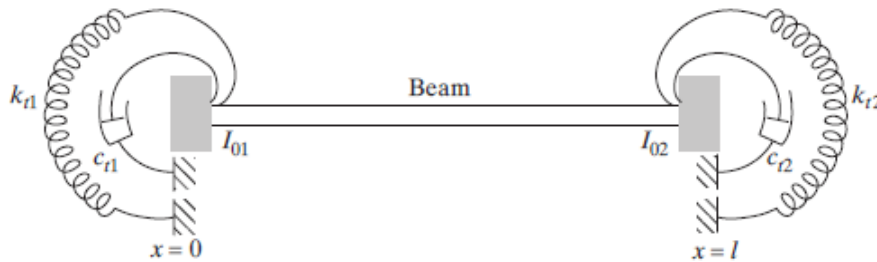
Figure A.9: Beam connected with torsional springs at its ends. Source:[12]

Appendix B

MATLAB scripts

B.1   MATLAB script for the knock of a hammer

```matlab
%% Script to record the knock of a hammer on the cylinder
%% Author: Eduardo Miranda
clear all;
close all;
clc;

% View available audio devices on the PC
d=daq.getDevices      % Get a list of the devices
info=audiodevinfo      % Returns information about the input and
    output
                       % audio devices on the system

% Get ID number of
info.input(2)          % Display the information on the input device 2

% Input Arguments
fs=44100;              % Sampling Frequency
nBits=24;              % Number of bits per sample
nChannels=1;           % Number of channels(mono or stereo)
ID=1;                  % Mic ID
n=15;                  % Number of seconds to record

% Record for n sec
recObj=audiorecorder(fs,nBits,nChannels,ID)
disp('Starting the Recording')
recordblocking(recObj,n);
disp('End of Recording');

% Store data and normalize it
y=-getaudiodata(recObj);
y=y/max(y);
```

```matlab
31
32  % Plot the recorded signal − Input 1/L
33  t=(0:length(y)−1)/fs;
34  figure;plot(t,y);
35  title('Impulse Response')
36  xlabel('Time (s)'); ylabel('Magnitude');
37
38  %% Welch's Method
39  WINDOW=512;              % Divides the signal into segments of 512
          samples
40  NOVERLAP=WINDOW/2;      % Number of overlapped samples (50%)
41  NFFT=2^16;             % Number of DFT points as integer
42
43  [pxx,F]=pwelch(y,hann(WINDOW),NOVERLAP,NFFT,fs);
44
45  %% Output
46  % Plot the spectrogram of the recorded signal
47  figure;spectrogram(y,WINDOW,NOVERLAP,NFFT,fs,'yaxis')
48
49  % Plot the frequency response with Welch's method
50  figure;plot(F,10*log10(pxx))
51  title('Frequency response')
52  xlabel('Frequency(Hz)'); ylabel('Magnitude(dB)');
```

B.2 MATLAB script for the linear verification of the system

```matlab
1  %% Script to confirm if the cylinder is an LTI system
2  %% Author: Eduardo Miranda
3  clear all;
4  close all;
5  clc;
6
7  % View available audio devices on the PC
8  d=daq.getDevices      % Get a list of the devices
9  info=audiodevinfo     % Returns information about the input and
       output
10                       % audio devices on the system
11
12 % Get ID number of
13 info.input(2)         % Display the information on the input device 2
14
15 % Input Arguments
16 fs=44100;             % Sampling Frequency
17 ts=1/fs;              % Sampling time
18 nBits=24;             % Number of bits per sample
19 nChannels=1;          % Number of channels(mono or stereo)
20 ID=1;                 % Mic ID
21 IDaudio=8;            % SoundBoard ID
22
23 % Sine wave
24 StopTime=5;           % Seconds to play the sine wave
25 t=(0:ts:StopTime-ts)';
26 n=StopTime+5;         % Seconds to record
27
28 %fc=1100;
29 fc=1500;
30 x=cos(2*pi*fc*t);
31
32 % Play Sine Noise
33 handler=audioplayer(x,fs,nBits,IDaudio)
34 play(handler)
35
36 % Record for n sec
37 recObj=audiorecorder(fs,nBits,nChannels,ID)
38 disp('Starting the Recording')
39 recordblocking(recObj,n);
40 disp('End of Recording');
41
42 % Store data and normalize it
43 y=-getaudiodata(recObj);
```

```matlab
44   [Y, I]=max( y ) ;
45   y=y/y ( I+10) ;
46
47   % PSD
48   N=length ( y ) ;
49   dft=fft ( y ) ;
50   dft=dft ( 1 :N/2+1) ;
51   psd =(1/( fs *N) ) * abs ( dft ) . ^ 2 ;
52   psd ( 2 : end −1)=2* psd ( 2 : end −1) ;
53   freq =0: fs / length ( y ) : fs /2;
54
55   %% Output
56   figure ; plot ( freq ,10 * log10 ( psd ) )
57   title ( 'Frequency  Response ' )
58   xlabel ( 'Frequency (Hz) ' )
59   ylabel ( 'Power/Frequency (dB/Hz) ' )
```

B.3   MATLAB script for the linear chirp

```matlab
1  %% Script to record the vibrations of the chirp on the cylinder
2  %% Author: Eduardo Miranda
3  clear all;
4  close all;
5  clc;
6
7  % View available audio devices on the PC
8  d=daq.getDevices      % Get a list of the devices
9  info=audiodevinfo     % Returns information about the input and
       output
10                       % audio devices on the system
11
12 % Get ID number of
13 info.input(2)         % Display the information on the input device 2
14
15 % Input Arguments
16  fs=44100;            % Sampling Frequency
17  ts=1/fs;             % Sampling time
18  nBits=24;            % Number of bits per sample
19  nChannels=1;         % Number of channels(mono or stereo)
20  ID=1;                % Mic ID
21  IDaudio=8;           % SoundBoard ID
22  WINDOW=512;          % Divides the signal into segments of 512
       samples
23  NOVERLAP=WINDOW/2;   % Number of overlapped samples (50%)
24  NFFT=2^16;           % Number of DFT points as integer
25
26 % Chirp signal
27  T=100;               % Chirp duration
28  n=T+10;              % Number of seconds to record
29  f0=20;               % Chirp initial frequency
30  f1=20000;            % Chirp final frequency
31  t=0:ts:T-ts;         % Time samples
32  x=chirp(t,f0,T,f1,'linear');
33
34 % Play Chirp noise
35  handler=audioplayer(x,fs,nBits,IDaudio)
36  play(handler)
37
38 % Record for n sec
39  recObj=audiorecorder(fs,nBits,nChannels,ID)
40  disp('Starting the Recording')
41  recordblocking(recObj,n);
42  disp('End of Recording');
```

```matlab
43
44  % Store data and normalize it
45  y=-getaudiodata(recObj);
46  [Y,I]=max(y);
47  y=y/y(I+10);
48
49  % Plot the recorded signal - Input 1/L
50  t=(0:length(y)-1)/fs;
51  figure;plot(t,y);
52  title('Recorded Signal')
53  xlabel('Time (s)'); ylabel('Magnitude');
54
55  figure;spectrogram(y,WINDOW,NOVERLAP,NFFT,fs,'yaxis')
56
57  %% Correlation techquinique
58  % Autocorrelation of the chirp signal
59  N=length(x);
60  Lag=4*fs;                    % Number of samples for the impulse
           response
61  Rxx=2*xcorr(x,x,Lag)/N;
62  n=-Lag:Lag;
63  figure;plot(n,Rxx,'b')
64
65  % Correlation with Err samples
66  Rxy=2*xcorr(y,x,Lag)/N;
67  hold on
68  plot(n,Rxy/max(Rxy),'r')
69  title('Correlated signals')
70  xlabel('Samples'); ylabel('Magnitude');
71  legend('Autocorrelation','Cross-correlation')
72  hold off
73
74  % Calculate the Error and correct it
75  [Y1,Irxx]=max(Rxx);
76  [Y2,Irxy]=max(Rxy);
77  Err=abs(Irxy-Irxx);
78
79  y=y(Err+1:end);
80
81  % Autocorrelation of the chirp signal
82  Lag=4*fs;                    % Number of samples for the impulse
           response
83  Rxx=2*xcorr(x,x,Lag)/N;
84  n=-Lag:Lag;
85  figure;plot(n,Rxx,'b')
86
87  % Correlation without Err samples
```

```matlab
88   Rxy=2*xcorr(y,x,Lag)/N;
89   hold on
90   plot(n,Rxy/max(Rxy),'r')
91   title('Correlated signals')
92   xlabel('Samples'); ylabel('Magnitude');
93   legend('Autocorrelation','Cross−correlation')
94   hold off
95
96   %% Output
97   % Create the digital filter to calculate its impulse and frequency
         response
98   h1=Rxy(Lag+1:end);
99
100  % Frequency response of a digital filter
101  [H1,f]=freqz(h1,1,NFFT,fs);
102
103  % Impulse Response of the whole signal
104  n1=(0:length(h1)−1)/fs;
105  figure;plot(n1,h1/max(h1))
106  title('Impulse Response')
107  xlabel('Time(s)'); ylabel('Magnitude');
108
109  % Spectrogram of the Impulse Response
110  figure;spectrogram(h1,WINDOW,NOVERLAP,NFFT,fs,'yaxis')
111
112  % Frequency Response of the whole signal
113  figure;plot(f,10*log10(abs(H1)),'r')
114  title('Frequency Response')
115  xlabel('Frequency(Hz)'); ylabel('Magnitude(dB)');
116
117  % Cut the start of the impulse response (0.5 seconds) to acquire
         the frequencies with a
118  % higher time span
119  h1=h1(fs/2:end);
120
121  % Impulse Response of the ''tail''
122  % n1=0:length(h1)−1;
123  n1=(0:length(h1)−1)/fs;
124  figure;plot(n1,h1)
125  title('Impulse Response')
126  xlabel('Time(s)'); ylabel('Magnitude');
127
128  % Spectrogram of the tail
129  figure;spectrogram(h1,WINDOW,NOVERLAP,NFFT,fs,'yaxis')
130
131  % Frequency response of a digital filter
132  [H1,f]=freqz(h1,1,NFFT,fs);
```

```matlab
133
134 % Frequency Response of the tail
135 figure; plot(f,10*log10(abs(H1)),'r')
136 title('Frequency Response')
137 xlabel('Frequency(Hz)'); ylabel('Magnitude(dB)');
```

References

[1] Dustin Mulvaney and Paul Robbins, Green Energy: An A-to-Z Guide. 2011

[2] H. P. Wu and Z. H. Yang, Liquid level detector for a sealed gas tank based on spectral analysis, Int. Conf. Digit. Signal Process. DSP, vol. 2014Janua, no. August, pp. 6872, 2014.

[3] Available:`https://hvacify.com/best-propane-tank-gauges-reviews/`[Acessed Nov. 14, 2018]

[4] A. S. Sovlukov and V. I. Tereshin, Radio-frequency measurement of liquefied petroleum gas mass in a tank, Autom. Remote Control, vol. 75, no. 9, pp. 17081715, 2014.

[5] X. Xu, Z. Li, G. Li, J. Li, and C. Wen, An Acoustic Resonance-Based Liquid Level Detector With Error Compensation, IEEE Trans. Instrum. Meas., vol. PP, pp. 19, 2018.

[6] M. I. Ilyasu and A. O. A, Ultrasonic Fluid Level Measuring Device, Int. J. Recent Dev. Eng. Technol. Website www.ijrdet.com, vol. 4, no. 1, pp. 23476435, 2015.

[7] M. H. Hayes, Statistical Digital Signal Processing and Modeling. 1996

[8] K. T. Chan and J. Z. Zhang, Free vibration of a cantilever tube partially filled with liquid, J. Sound Vib., vol. 182, no. 2, pp. 185190, 1995.

[9] K. T. Chan, T. P. Leung, and W. O. Wong, Free vibration of simply supported beam partially loaded with distributed mass, J. Sound Vib., vol. 191, no. 4, pp. 590597, 1996.

[10] M. A. Jacobs, R. Breeuwer, M. F. Kemmere, and J. T. F. Keurentjes, Contactless liquid detection in a partly filled tube by resonance, J. Sound Vib., vol. 285, no. 45, pp. 10391048, 2005.

[11] P. Kelly, Solid Mechanics Lecture Notes - An Introduction to Solid Mechanics. Auckland: The University of Auckland. 2013.

[12] S. S. Rao, Mechanical Vibrations, vol. 67. 2010.

[13] S. W. Smith, The Scientist and Engineer's Guide to Digital Signal Processing. 1999.

[14] J. G. Proakis and D. G. Manolakis, Digital Signal Processing: Principles Algorithms and Applications. 1996.

[15] J. H. McClellan, R. W. Schafer, and M. A. Yoder, DSP First. 2016.

[16] Available:`https://en.wikipedia.org/wiki/Chirp`[Acessed Oct. 10, 2018]

[17] E. C. Ifeachor and B. W. Jervis, Digital Signal Processing: A Pratical Approach. 1993.

[18] Available:`https://docs.scipy.org/doc/scipy/reference/generated/scipy.signal.fftconvolve.html`[Acessed Oct. 10, 2018]

[19] Jorge Miguel da Costa Cubal, "Fortius IV - Posicionamento de Microfones," 2010.

[20] Available:`https://www.roland.com/uk/products/fa-66/specifications/`[Acessed Nov. 3, 2018]

[21] Behringer, "Measurement Microphone ECM8000," ECM8000 datasheet, July 2000.

[22] S. L. Marple, Digital Spectral Analysis with Applications. 1987

[23] Vibe-Tribe Ninja 3D speaker User Manual, Unicorn Srl, Italy, 2011